https://doi.org/10.48048/tis.2024.8759

A Review of Rare Earth Ion-Doped Glasses: Physical, Optical, and Photoluminescence Properties

Serifat Olamide Adeleye[1], Adekunle Akanni Adeleke[2,*], Petrus Nzerem[3], Adebayo Isaac Olosho[4], Esther Nneka Anosike-Francis[2], Temitayo Samson Ogedengbe[2], Peter Pelumi Ikubanni[5], Rabiatu Adamu Saleh[1] and Jude Awele Okolie[6]

[1]Department of Industrial Chemistry, Nile University of Nigeria, Abuja, Federal Capital Territory 900108, Nigeria
[2]Department of Mechanical Engineering, Nile University of Nigeria, Abuja, Federal Capital Territory 900108, Nigeria
[3]Department of Petroleum and Gas Engineering, Nile University of Nigeria, Abuja, Federal Capital Territory 900108, Nigeria
[4]Department of Petroleum Chemistry, American University of Nigeria, Yola, Nigeria
[5]Department of Mechatronics Engineering, Bowen University, Road, Ogun State 112107, Nigeria
[6]Gallogly College of Engineering, University of Oklahoma, Norman, OK 73019, United States

([*]Corresponding author's e-mail: adeleke.kunle@ymail.com)

Received: 29 July 2024, Revised: 19 August 2024, Accepted: 26 August 2024, Published: 20 October 2024

Abstract

Researchers worldwide have shown significant interest in doping glasses with rare-earth ions. This is particularly intriguing because rare-earth ions are extensively used to enhance the optical properties of host glasses, capitalizing on their unique spectroscopic characteristics due to optical transitions within the intra-4f shell. An in-depth review was conducted on various glass fabrication methods, such as sputtering, sol-gel, chemical vapor deposition, ion exchange, and direct melt quenching. The study emphasized the physical, optical, and photoluminescence properties of glasses made from glass formers co-doped with rare-earth ions. Understanding the interrelationship between these properties is crucial for optimizing material performance across various technological applications. The research highlights the broad applicability of rare-earth-doped glasses in fields like white light emission, photonic devices, solid-state lasers, optical fiber communication, and biomedical applications

Keywords: Rare earth ions, Laser, Photonics, Melt-quenching, Light emitting diode, Radiative properties, Photoluminescence, Physical properties

Introduction

In recent years, experts have been interested in conducting comprehensive research on glasses doped with rare-earth ions (REIs). Doping glasses with REIs have become essential for many industrial processes Shaaban *et al.* [1] and the advancement of devices for homes and businesses in developed nations [2]. REIs are often referred to as "the vitamins of modern industry" due to their frequent use in improving the optical and physical attributes of host glasses, which find applications in various personal gadgets like mobile phones, laptops, and televisions Balaram [3], as well as 3-dimensional (3D) displays Shaaban *et al.* [1], medical diagnosis, drug delivery Naseer and Marimuthu [4], fiber optics Goodenough et al. [2] and wastewater treatment Limpichaipanit *et al.* [5], among others. Since the latter part of the 20th century, the development of REI-doped glasses for laser and amplifier production has shown promise [6]. Glass is an amorphous solid that possesses significant properties that make it a fundamental material with numerous potentials across various sectors. It lacks a long-range and periodic atomic structure [7]. Despite the increasing demand for glass, the availability of its primary raw materials is diminishing over time.

REIs stand out from other ions with optical activities due to several distinctive features, especially the trivalent form. They exhibit emission and absorption within restricted wavelength ranges, their emission and absorption wavelengths are mainly unaltered by the host material, they possess low magnitude, long lifetimes of metastable states, and high quantum efficiencies [8]. These properties make REIs highly suitable for numerous optical applications as depicted in **Figure 1**.

The addition of REIs to glasses enables the observation of well-defined spectral lines of absorption and emission, resulting from electronic changes that take place within the ions' $4f^n$ shell configuration. Moreover, the positions of these spectral lines are minimally influenced by the surrounding environment due to the effective shielding of the *f* shell from external ligands [9]. The host material that contains the REIs primarily influences the intensities of these lines. Glasses doped with REIs are the preferred medium for all-solid-state lasers because they emit visible and near-infrared (NIR) lasers more efficiently than single crystals [2,10]. Glass photoluminescent properties are significantly enhanced and modified by REIs. They function incredibly well as luminescent centers because of their distinct electronic structure. The effects of REI on photoluminescence include the production of narrow emission bands, unique emission properties resulting from specific energy level transitions, and high quantum efficiency that is, the ability to absorb photons and re-emit them with minimal loss. Compared to other dopants, the photoluminescence process becomes more efficient because it can transfer energy through a process known as sensitization. In both the visible and UV spectrums, it possesses distinct absorption bands. The excitation energy is absorbed by the sensitizer ion and transferred to the activator ion, which releases light. The quest for novel glass materials possessing high quantum efficiency that can incorporate REIs and manipulate their luminescence characteristics through the modification of the environment is therefore important.

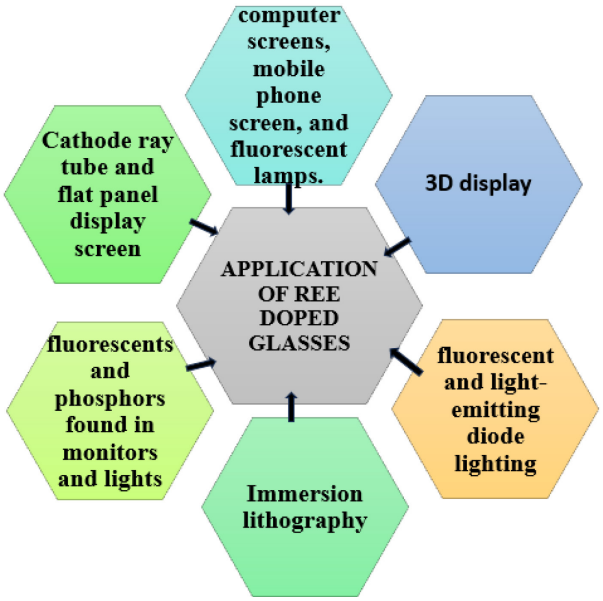

Figure 1 Application of REE-doped glasses.

The physical properties of glass, such as refractive index and density, can be altered by incorporating various chemical constituents known as network modifiers. A deep understanding of the fundamental structure of different glass network formers is essential to grasp the role of these modifiers. Glass, as a material, offers ease of manufacturing and uniformity, making it an ideal host for rare-earth ions (REI), particularly when it has a low non-linear refractive index and maintains a consistent concentration of dopants. Moreover, the abundance, large-scale production potential, chemical resistance, and thermal stability of oxide glasses make them well-suited for a wide range of applications without significant risks. [4].

This review focuses on selected glass compositions doped- $Sm^{3+,}$ Er^{3+}, and Er^{3+}/Yb^{3+} and aims to provide valuable insights and contribute to advancements in this field by thoroughly analyzing the optical and physical properties of glasses doped with REIs.

Fabrication techniques of glasses doped with rare earth ion

Glass is a material with numerous applications that is both adaptable and widely used from everyday objects like windows and bottles to advanced technologies such as optical fibers and precision optics. The diversity of glass applications is due in large part to the various fabrication methods available for shaping and forming glass into desired forms. Glass fabrication typically begins with the melting of raw materials, which include calcium carbonate ($CaCO_3$), sodium carbonate (Na_2CO_3), and silica (SiO_2), along with other additives for specific properties. Melting of raw materials is then followed by Shaping and refining of the glass [11]. **Figure 2** illustrates a thorough glass manufacturing process.

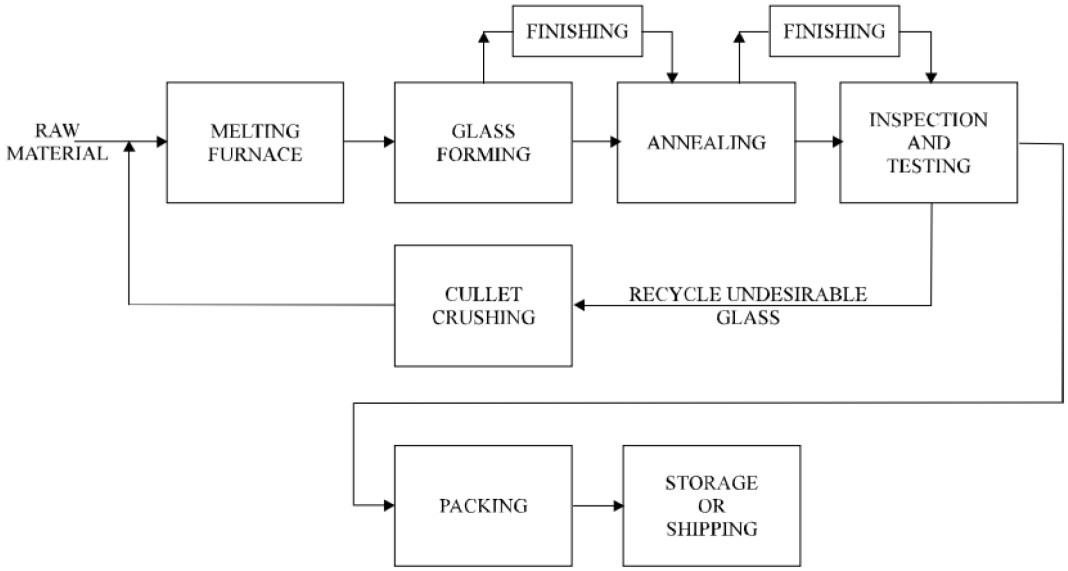

Figure 2 Typical glass manufacturing process [11].

Glass fabrication involves a wide range of methods, each tailored to specific applications and desired properties. From ancient glassblowing techniques to cutting-edge processes for producing optical fibers and precision optics, glass's versatility and adaptability to various fabrication methods continue to drive innovation and enable a multitude of essential and advanced technologies. Understanding these fabrication methods is crucial for harnessing glass's full potential in a myriad of applications.

Rare earth ions have become attractive materials for scientists and engineers due to their exceptional optical and luminescent properties. A glass sample can also be co-doped with rare-earth ions (REIs), which involves introducing additional dopants or modifying REIs within the glass matrix to alter its structural and optical characteristics. Post-processing techniques, such as heat treatment and annealing, can further enhance the glass's luminescent properties [12,13]. When these ions are integrated into glass matrices, they open a realm of possibilities for applications ranging from telecommunications and laser technologies to advanced optics and lighting systems. Several methods are employed to introduce REI into glass matrices, each offering distinct advantages and tailored to specific applications.

Many factors and conditions can greatly influence the fabrication of glass materials with optical, physical, and photoluminescence characteristics. **Table 1** displays these parameters.

Table 1 Glass preparation parameters and conditions.

Parameters	**Conditions**	References
Concentration of glass component	A glass's optical, photoluminescence, and physical characteristics are largely dependent on the concentration of its components. the qualities of a glass sample, for example, are typically influenced by the network former (such as silica) and network modifier (such as dopant). A glass sample's refractive index, absorption, and	[4]

Parameters	Conditions	References
	transmittance are all influenced by glass components when it comes to optical properties. It may cause a glass wavelength and intensity to shift. Additionally, the concentration of the glass's constituents affects its density, i.e when heavy atoms replace lighter ones like boron, the density of the glass increases.	
Melting temperature	The high temperatures during the melting process can enhance crystallinity and minimize defects, though it may also cause the grains to become coarse. As an illustration, higher melting temperatures in chemical vapor deposition (CVD) have the potential to yield better graphene quality, but they also increase the possibility of unintended phase changes	[14]
Annealing process/post-heating treatment	High temperatures during the annealing process or post-treatment may improve crystallinity and decrease defects, resulting in sharp optical absorption edges and improved photoluminescence. prolonged annealing periods can improve material structure even more; however, they can also cause unexpected phase transitions or sintering	[15,16]
Cooling	Rapid cooling of a sample of glass could result in the creation of amorphous structures or metastable phases, which could alter the optical properties. To attain the desired crystal phases and enhance optical quality, controlled cooling rates can be advantageous.	[15,16]

Direct melt quenching method

The direct melt quenching method is a conventional technique that involves the rapid cooling of molten substances such as SiO_2 (silicate), BeF_2 (beryllium fluoride), B_2O_3 (borate), As_2O_3 (arsenic trioxide), P2O5 (phosphate), and GeO_2 (germanium oxide). This process results in the formation of an amorphous solid, which lacks long-range order. The rapid cooling significantly increases the viscosity of the molten liquid, preventing atomic rearrangement and leading to the creation of an amorphous structure. Unlike crystalline materials, the spatial arrangement of atoms and ions in an amorphous solid does not exhibit the typical 3-dimensional periodicity and long-range order [12].

This method is widely used in the fabrication of bulk glasses, optical fibers, and the development of gain media for lasers. For example, in a study by Sushama and Predeep [13], rare earth-doped tungsten-tellurite glasses were prepared using this method, employing an alumina crucible in an ambient air atmosphere. The resulting glass demonstrated remarkable stability at high temperatures, and it was observed that the addition of rare-earth ions (REIs) decreased the optical band gap. The investigation of optical properties at the laboratory scale is a straightforward application of this glass formation technique. For instance, Dousti *et al.* [17] used this method to produce tellurite glass embedded with silver

nanoparticles and doped with Eu^{3+} ions, as shown in **Figure 3**. Their study found that the presence of silver nanoparticles enhanced the luminescence of Eu^{3+} ions.

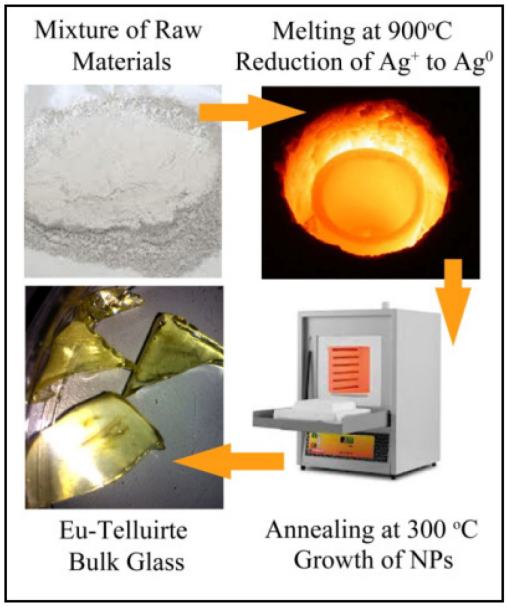

Figure 3 Schematic phases involved in preparing glass using the melt-quench method [17].

Sol-Gel technique

In the middle of the 1800s, the sol-gel method became a ground-breaking substitute for conventional glassblowing methods. This chemical synthesis method, conducted in aqueous media, proved highly effective for crafting glasses at lower temperatures [18]. The process commences with the formation of a sol, constituting a colloidal suspension primarily composed of silica-based precursors. Subsequently, the sol undergoes gelation and is subjected to low-temperature heat treatment, ultimately yielding a solid glass product [19].

These precursors are made up of substances that contain REIs. These components can be found in these precursors in a variety of forms, including oxides, alkoxides, carboxylates, nitrates, and chlorides. Selecting a precursor depends on several factors, including the desired doped glass properties, the particular REIs needed, and the overall conditions of the sol-gel process. Precursors that enable the smooth incorporation of REIs into the sol-gel matrix and ensure the required degrees of purity and uniformity in the finished glass material are frequently chosen by researchers. Many alkoxides are highly versatile and, as a result, are often used in the preparation of inorganic solids because of their broad solubility in organic solvents, especially alcohols. Water, alcoholic solvents, catalysts (base or acid), and alkoxide precursors, such as Si (OCOC2H5), are commonly used in procedures involving these precursors. The hydrolysis of the alkoxide starts the process and produces monomers that can take part in condensation reactions and form aggregates. The size of these aggregates steadily grows until they fill the entire volume of the solution, forming a 3-dimensional (3D) network that represents the change from a “sol” phase to a “gel” phase. **Figure 4** illustrates this procedure, with R standing in for C_2H_5. [19].

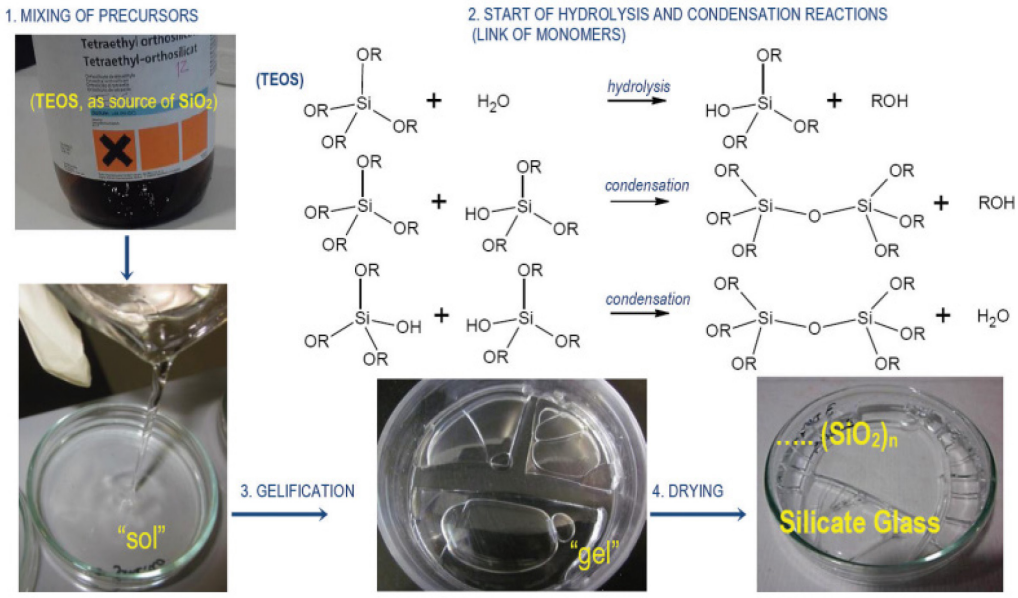

Figure 4 Scheme of the evolution of sol-gel-glass [19].

Sharifianjazi *et al.* [20] used sol-gel techniques in an ambient environment to synthesize SiO_2–CaO–P_2O_5–Ag_2O bioactive glass (BG). Following an immersion in simulated body fluid (SBF), the composition showed improved biocompatibility and the production of hydroxylapatite.

To coat titanium grade 4 substrates with a layer of calcium silicate glass, Catauro *et al.* [21] utilized the sol-gel method to create glasses with increasing concentrations of silver oxide. However, it has been noted that coatings with high Ag contents exhibit a slight decrease in both bioactivity and biocompatibility. In contrast, the films' ability to combat Staphylococcus aureus bacteria grows as the amount of silver in them increases. According to the findings, coatings with high silver percentages have negative biological effects.

Monolithic and thin-film nanocomposites of alumina phosphate glasses were synthesized via the use of a modified sol-gel process by Battisha *et al.* [22]. The glass samples were activated by doping with 3 different REIs (Er^{3+} Yb^{3+} Sm^{3+}). Thin film samples, as opposed to monolithic ones, reportedly had their crystallite sizes decrease from 44 to 31 nm upon triply doping the prepared glass samples with Er^{3+}, Sm^{3+}, and Yb^{3+} ions. It is observed that the ions Er^{3+} and Sm^{3+} have a small absorption cross-section. Consequently, Yb^{3+} ions are employed as a sensitizer to improve the PL emission of Er^{3+} and Sm^{3+} ions while offering a good spectral overlap with the transition between Er^{3+} and Sm^{3+}. Er^{3+} emission is facilitated by this efficient energy transfer between Yb^{3+}, $Er^{3+,}$ and Sm^{3+}.

Ion-exchange and sputtering techniques

This process infuses glass surface layers with REIs. While sputtering entails bombarding the glass surface with high-energy ions, which causes the emission and incorporation of REIs, ion exchange depends on the diffusion of ions from a molten salt bath into the glass. Sgibnev *et al.* [23] explored the growth processes of silver clusters and nanoparticles in antimony-doped PTR glasses under UV excitation at 365

nm. They found that silver clusters in Sb-doped PTR glasses exhibit strong broadband emission in the 400 - 950 nm range, offering new possibilities for their use as phosphors in white LEDs and down-converters for solar cells. Varak *et al.* [24] prepared a series of zinc-silicate glass samples doped with Ho^{3+}/Yb^{3+}, Er^{3+}/Yb^{3+}, and Tm^{3+}/Yb^{3+} ions. Using the ion-exchange method, co-doped of the glass samples with silver to improve the glass's silver content was carried out. After that, different heat treatment procedures were used to cause silver to materialize as silver ions, dimers, or metallic silver nanoparticles, among other oxidation states and forms. The result showed that the energy-transfer mechanism of silver dimers enhances the luminescence of REI-doped glass upon excitation in the visible range. Furthermore, when a silicate matrix underwent structural changes and the SPR (surface plasmon resonance) effect of silver nanoparticles came together, an increase in photoluminescence was observed at 975 nm upon excitation. **Table 2** displays a comparison of the various methods used in the fabrication of REI-doped glasses.

Table 2 Advantages and limitations of different fabrication techniques of REI-doped glasses.

Glass fabrication techniques	Advantages	Limitation
Melt-quenching method [23]	• Modifier oxide does not always need to be added excessively to reduce processing temperature. • size, shape, and quantity of its components, as well as its availability system • Its composition is extremely versatile. which forms the basis for the most important industrial glasses, including various glass lasers, color filters, etc.	• Due to the high melting temperature required for this technique, preparing glasses containing large amounts of refractory material, such as SiO2, titanium dioxide (TiO_2), alumina (Al_2O_3), zirconium oxide (ZrO_2), etc is very challenging. • The challenge of preserving optimal purity also pertains to potential contamination from materials in the furnace or crucible, which usually react with the glass melt at high temperatures
Sol-gel [24]	• Produce glasses of ultra-high purity. • It is cheaper, easier, and more homogenous, particularly for multicomponent glasses. • Achieving a high doping level of rare earth ions in silica glass while	• With this method, high OH- ion content is its primary optical property limitation. This type of material's constant OH bonds act as powerful energy quenchers for the rare earth ions,

Glass fabrication techniques	Advantages	Limitation
	minimizing the formation of rare earth ion clusters is feasible.	causing an extremely short lifetime in the excited state. This lowers the likelihood of stimulating emitted photons
chemical vapor deposition (CVD) [23]	• making extremely pure glasses • generates high-purity silica glass that is used in many kinds of optical and optoelectronic devices.	• Glasses doped with alkali and alkaline earth elements, or those that contained REI, cannot be produced by this technique.
Ion-exchange and sputtering [23]	• It Produces Glass strengthened Chemically • The glass's chemical and physical properties can be altered with cheap technology	• In large-scale production, the procedure can be expensive and time-consuming. • Not every glass composition can be suited for ion exchange, and not every material can be sputtered easily

Properties of REI doped glasses

Optical and physical properties REI-doped glasses

Density is a fundamental physical property providing information about the compactness and mass distribution within a glass volume. Density is a key factor in determining a sample's molar volume, refractive index, and polarizability, among other attributes. It represents how tightly the particles or molecules of glass are parked together [25]. The density and molar volume of various REI-doped glasses are presented in **Table 3**.

Table 3 Summary of the previous studies on physical properties of REI-doped glassesss.

Glass composition	Rare earth used	Major finding (density and molar volume trends)	References
$(Bi_2O_3+B_2O_3+SiO_2+Er_2O_3)$ glasses	Er^{3+}	Density: Increases Molar volume:	[26]
$\{[(B_2O_3)_{0.3}\ (TeO_2)_{0.7}]_{0.8}\ (SiO_2)_{0.2}\}1-x\ (Er_2O_3)x$	Er^{3+}	Density: Increases Molar volume:	[27]
$50SiO_2$ -$30Li_2O$- $1Gd_2O_3$- (19 − x)CdO	Er^{3+}	Density: Increase from 3.12 to 3.57 molar volume: Iecreases, 21.5 - 20.5	[1]

Glass composition	Rare earth used	Major finding (density and molar volume trends)	References
(60-x)Bi_2O_3:10PbO:10Li_2O:20SiO_2:xPm_2O_3 (LLBS)	Pm^{3+}	Density: Increase (3.155 - 3.586) molar volume: Iecreases (100.074 - 90.122)	[28]
10ZnO–5Na_2O–10Bi_2O_3–(75−x) B_2O_3–xEu_2O_3 ((ZnNaBiB))	Eu^{3+}	Density: Increases (3.498 - 3.701) Molar volume: Increase (31.945 - 32.493)	[29]
10SiO_2–10Al_2O_3–(40-x-y)B_2O_3–30ZnO–10Li_2O–xEr_2O_3– yYb_2O_3,	Er^{3+}/Yb^{3+}	Density: Increases (3.623 - 3.758) Molar volume: Increases (21.032 - 22.008)	[30]
65B_2O_3–(35 - 2x)PbO–xSm_2O_3–xGd_2O_3	Sm^{3+}/Gd^{3+}	Density: Decreases (4.650 - 4.502) Molar volume: Increases (26.82 - 28.87)	[25]
40 Li_2O- 05BaO- 05Gd_2O_3- (50-x) SiO_2:x Sm_2O_3 (LBGS)	Sm^{3+}	Density: Increases (2.985 - 3.103) Molar volume increases (22.713 - 23.707)	[31]

Incorporating rare-earth ions (REIs) into glass structures significantly alters their physical properties, such as molar volume and density, which may increase or decrease depending on the specific changes. Hegde *et al.* [29] reported that the increase in glass density and mean molecular weight could result from the substitution of lighter atoms in the network with heavier REI atoms. An increase in density may also lead to changes in the glass's cross-link density. Additionally, the incorporation of REIs can break network bonds, leading to the formation of non-bridging oxygen (NBO). This indicates that during the glass-making process, REIs act as network modifiers, contributing to the breaking of bonds and the creation of NBOs [26,34].

Reports by Acikgoz *et al.* [35] and Khan *et al.* [31] indicate that density increases with higher concentrations of rare-earth ions (REIs), suggesting stronger bonding between atoms and atomic groups within the glass network. Conversely, reduced density in glass samples with increasing REI concentrations may be attributed to shorter atomic bonds or smaller interatomic spacing. Additionally, this decrease in density reflects the formation of non-bridging oxygens (NBOs), which contribute to the lower density of the glass sample. The reduction in density further confirms that the glass network becomes more loosely packed as the concentration of rare-earth oxides increases [25].

The physical properties of glass are significantly influenced by the oxygen packing density (OPD), which is a crucial parameter for understanding the compactness of the oxide network. The OPD of the glass network is directly related to several properties, including the refractive index, molar volume, density, microhardness, and glass transition temperatures. Both the composition of the glass and the presence of network formers and modifiers affect the OPD. Research has shown that higher OPD values are associated with greater network cross-linking, and an increase in density reflects both a rise in OPD and a reduction in the number of non-bridging oxygens (NBOs) in the glass matrix [36].

According to Meena *et al.* [28], molar volume and density typically exhibit inverse behavior. Molar volume is directly related to bond length, with an increase in bond length leading to a larger molar volume, which indicates a more loosely packed glass network. Minor variations in molar volume may result from changes in the coordination of rare-earth ions and the composition of the glass network [1,28]. However, in certain cases, such as with LGBS and RHSBT [37], molar volume increases with the density of glass samples as REI concentration rises. This unusual behavior may be due to the formation of non-bridging oxygens (NBOs), which expand the structure of the glass network. The creation of excess free volume, due to the larger radii and bond lengths of REIs compared to the glass composition, leads to an increased total molar volume [30,38].

Polarion radius (r_p), interionic distance (r_i) and field strength (F_s)

The term polaron radius describes the linear atomic or ionic displacement field associated with polaron. A polaron is considered small if its radius is comparable to the lattice constant, while a large polaron has a radius much larger than the lattice constant of the material. The strength of attraction between cations and anions in an ionic compound is determined by the interionic distance, which is the distance between the centers of 2 ion nuclei. Increasing the concentration of rare-earth ions (REIs) typically leads to a decrease in the interionic distance and an increase in the field strength of the glass due to a higher ion density per unit volume [39]. As REI concentration rises, the polaron radius and interionic distance tend to decrease, which explains the higher values of (N) for REIs. The reduced average distance between rare earth ions and oxygen results in stronger bond formations around the REI ions. This observation is consistent with patterns seen in other reported structures, such as LLBS Meena [28], ZnNaBiB-Eu Hegh *et al.* [29], BLFBEr Mariselvam *et al.* [39], and ZnAlBiB-Dy glasses [40].

Metallization criterion

The measure of a material's metallic or insulating attributes is the metallization criterion. If the metallization criterion value of glass materials increases, they are considered to have insulating behavior; if it declines, they are regarded to have metalizing behavior. based on the metallization theory proposed by Herfeild [41]. According to Halimah *et al.* [42], the metallization criterion is given as $1 - {}^{R_m}/_{V_m}$, if ${}^{R_m}/_{V_m} > 1$ (metal) and ${}^{R_m}/_{V_m} < 1$ (non-metal). The metallization criterion depends on the band gap energy and refractive index to determine the nature of solids Kashif *et al.* [43] according to Eq. (5).

$$M = 1 - \left[\frac{n^2-1}{n^2+2}\right] = \sqrt{\frac{E_g}{20}} \quad (5)$$

Dimitrov *et al.* [44] observed that a decrease in the energy gap and an increase in the linear refractive index can be attributed to increased metallicity and a higher nonlinear refractive index. A decrease in the energy gap is linked to a reduction in the metallization criterion. As the metallization criterion becomes smaller, the valence and conduction bandwidths expand, resulting in a narrower band gap [45]. Scholars have found that the metallization criterion of some rare-earth ion (REI)-doped glasses decreases with increasing REI concentration, leading to both an increased refractive index and a reduced band gap energy. This suggests that the glass material is becoming more metallic, as indicated by the decreasing metallization criterion [28,46]. However, for some glass samples, an increase in REI concentration can also lead to an increase in the metallization criterion. Despite the increasing band gap energy and refractive index, the decreasing metallization criterion suggests a lower tendency for metallization in the electronic structure. An upward trend in the metallization criterion based on band gap energy indicates that the samples are not becoming metallic, and the conduction band width is decreasing [42,47].

Polarizability of oxide ions and optical basicity

The properties of oxides, glasses, alloys, slags, molten salts, and other acid-based materials are described in detail using optical basicity values [46]. The oxide ion polarizability can be determined from the band gap energy and refractive index [48]. It is well established that materials with higher oxide ion polarizability exhibit a higher refractive index. El-Maaref *et al.* [49] introduced the concept of optical basicity to measure the acid-base properties of oxide glasses. In this framework, the metal ion is considered acid, while oxygen acts as the base. The optical basicity of oxide glasses can be calculated based on the oxide ion polarizability using the Duffy method, as outlined in Eq. (6) [50].

$$\Lambda_n = 1.67\left(1 - \frac{1}{\alpha_{O^{2-}}}\right) \quad (6)$$

Eq. (6) indicates that as polarizability increases, so does optical basicity, and this ultimately causes the refractive index to increase. Electronegativity was employed by Zhao *et al.* [80] and Reddy *et al.* [56] as an alternative method for a few glasses that Dimitrov and Komatsu had previously examined. Zhao *et al.* [80] proposed optical electronegativity, which is computed from the refractive index and expressed as Eq. (7), to estimate oxide glasses' ability to polarize oxide ions.

$$\alpha_{O^{2-}} = 3.5 - 0.9\chi_{\text{glass}} \quad (7)$$

The average electronegativity and oxide ion polarizability are strongly correlated, according to Reddy et al. [56] and Moustafa and Elkhateb [55]. The optical basicity of glass samples can be estimated using Eq. (8) [1].

$$\Lambda = 1.7 - 0.5\chi \quad (8)$$

In some cases, the refractive index and oxide ion polarizability, based on the energy band gap, exhibit the same trend, whether increasing or decreasing. For instance, as the concentration of rare-earth ions (REIs) increases in the glass system, the amount of non-bridging oxygens (NBOs) with high polarizability decreases, leading to a downward trend [42]. Higher optical basicity in oxide ions enhances their ability to transfer electrons to adjacent cations. During the acid-base modification reaction, when REIs are added to the glass, the modifier oxide ions migrate towards the more acidic region of the original oxide, decreasing in acidity. An increase in optical basicity indicates a reduction in covalency [43].

Optical parameters of REI-doped glasses

Absorption spectra analysis is crucial for determining various optical properties of materials, including transmission losses, absorption cross-sections, and the refractive index. The intensities of absorption bands can be expressed in terms of oscillator strengths. **Figure 5** illustrates the room temperature absorption spectra of Er3+-doped bio-silicate borotellurite glass in the UV-VIS-NIR range, as reported by Hamza e*t al.* [53]. The Er3+ ions exhibit electronic transitions from their ground state $^4I_{15/2}$ to various excited states, resulting in the distinct absorption bands shown in **Figure 5**.

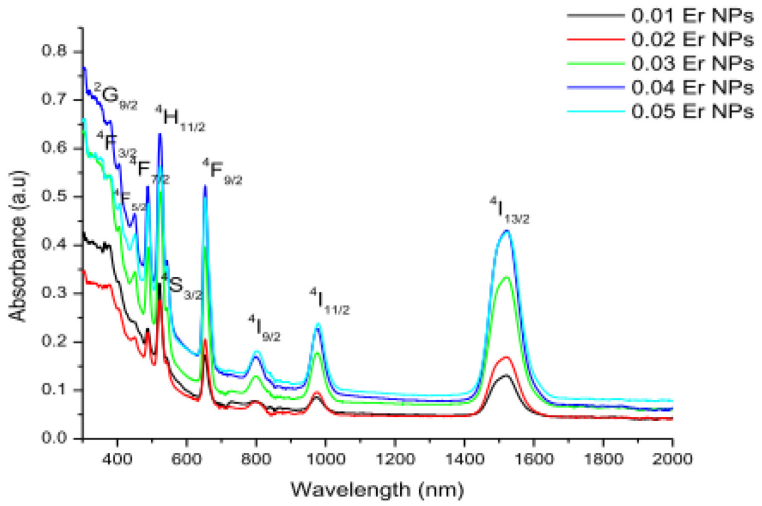

Optical band gap energy (E_g) ***and urbach energy*** (ΔE)

The optical band gap energy is a crucial characteristic of solid-state laser materials [53,54]. The optical absorption spectrum is a key tool for understanding the optical band gap, as it provides insights into the electronic structure of the amorphous material [39]. To measure the optical band gap, electrons are excited from the top of the valence band to the bottom of the conduction band using photons of specific

frequencies. This measurement significantly aids in understanding the electronic structure and bonding within the glass network [55]. The optical band gap is calculated using Tauc's empirical model [56].

The addition of rare-earth ions (REIs) to glasses has sometimes been observed to increase the indirect band gap. This increase is often attributed to a reduction in non-bridging oxygens (NBOs) due to structural changes within the glass system [42,33,57]. Another possible explanation for the increased optical band gap is the enhanced rigidity of the glass system following REI incorporation. Some researchers have noted an upward trend in the band gap with increasing REI concentration. However, structural changes induced by REIs, such as the formation of additional NBOs, can lead to an increase in free electrons, which may contribute to a decrease in the optical band gap [54,58,38]. Therefore, the modifications to the glass structure caused by the addition of a modifier influence the optical band gap for both direct and indirect transitions.

Urbach energy (ΔE) refers to the width of the localized states associated with optical transitions between localized tail states in the valence band and extended states in the conduction band above the mobility edge [47]. To determine the Urbach energy (ΔE) of a glass sample, one takes the reciprocal of the slope of the linear portion of the plot relating photon energy to lnα. Urbach energy measures the level of disorder within glass materials, which varies with the development of structural defects. Incorporating rare-earth ions (REIs) into glasses generally leads to a decrease in the level of disorder, as indicated by a lower Urbach energy [47]. Conversely, an increase in Urbach energy suggests a higher level of disorder in the glass network.

Electronic polarizability (α_m), molar refraction (Rm), and refractive index n

The refractive index (n) is a key optical parameter that describes how electromagnetic waves propagate through a material and how light interacts with it [55]. The refractive index of a glass sample can be calculated using the optical band gap, as determined by Tauc's method [25]. Generally, a glass with ions of similar polarizability will have a higher refractive index if its molar volume is smaller. The refractive index and other optical parameters can be determined using both the direct and indirect band gaps. As the band gap decreases, the refractive index tends to increase. Additionally, there is a relationship between the refractive index and the density of the glass sample [42]. A glass sample's refractive index (n) may increase or decrease in response to an increase in REI. For the following reasons, some glass samples have a higher refractive index:

1) The formation of non-bridging oxygens (NBOs) increases ionic bonds over the predominantly covalent bonds of bridging oxygen, leading to greater polarizability. When these NBOs interact with loosely bound rare-earth ions (REIs), the cohesiveness of the glass network decreases. NBOs, being more polarizable than bridging oxygens (BOs), enhance the polarizability and refractive index of glass samples. Thus, there is a direct proportionality between the refractive index and polarizability [34,38].

2) The incorporation of REIs into the glass matrix results in a denser packing of rare-earth modifiers within the host material, which contributes to an increased refractive index [36,38]. As the density of the packing network increases, so does the refractive index of the glass.

Compared to bridging oxygens (BOs), non-bridging oxygens (NBOs) are more polarizable, which increases the refractive index of the glass [46]. A reduction in the refractive index may occur due to the addition of modifiers that decrease the number of NBOs. As the content of rare-earth ions (REIs) increases, the refractive index tends to decrease because fewer high-polarizability NBOs are present [42]. The total polarizability of a material is reflected in its molar refraction, which is related to the molar polarizability [42,45]. The Lorentz-Lorenz equation connects the molar volume, refractive index, and molar refraction of the glass. In amorphous materials like pure glass, electronic polarization is the primary type of polarization, and electronic polarizability measures the electron response to an electric field [38].

As NBOs increase, their higher polarizability tends to raise the refractive index. This is due to NBOs having greater polarization potential compared to BOs [30]. The Clausius-Mosotti relation links the glass structure to its molar refraction, which is proportional to the material's molar electronic polarizability [38]. Changes in the molar refraction and polarizability of the glass are evident with increasing REI content. The increase in NBOs within the glass system contributes to this trend, as NBOs are more polarizable than BOs. Typically, glasses with higher concentrations of NBOs exhibit greater polarization and, consequently, a higher refractive index [25,36,46,59]. Conversely, a decrease in BOs may result in a lower refractive index [42]. Therefore, the polarizability of the glass affects its refractive index beyond just density. Glasses with a higher refractive index also tend to have higher polarizability and molar refraction. **Table 4** compares the ionic polarizability, refractive index, and molar refraction of various documented glasses.

Table 4 Comparison of refractive index (n), polarizability (αm), and molar refraction (Rm) of some glasses.

Research title	Molar refraction (R_m)	Refractive index (n)	Polarizability (α^3)	Major finding	Source
Polarizability and optical fundamentality of glasses doped with Er^{3+} ions in tellurite	Increase	Increase	increase	This increase suggests that the material is becoming more polarized due to an increase in NBOs.	[46]
Zinc borotellurite glass doped La^{3+} ions: optical basicity and electronic polarizability	Decrease	Decrease	decrease	There is a trend toward a decrease in the quantity of nonbridging oxygen with high polarizability as the concentration of REI increases in the glass system	[42]
properties of rice husk silicate borotellurite (Erbium-doped RHSBT) glasses in	Increase	Decrease	increase	The observed increase in polarizability is explained by the greater polarizability of Er^{3+} ions compared to TeO^{4+}	[27]

Research title	Molar refraction (R_m)	Refractive index (n)	Polarizability (α^3)	Major finding	Source
terms of morphology, structure, and optics				ions that have been substituted in the glass network	
Optical, Polarizability, basicity, and optical properties	Increase	Increase	increase	The increase in these parameters' values is attributed to the glass system's large atomic weight, high Bi^{3+} polarizability, and coordination number of Bi_2O_3	[43]
Studies of Erbium-Doped Borosililicate Glass: Physical and Optical	Decrease	Decrease	decrease	Refractive index and molar refraction at 2.0 mol % increase as a result of the dense packing of RE modifiers into the host materials brought about by the inclusion of REI in the network. In contrast, high polarity is the cause of the increase in polarizability at 2.0 and 4.0 mol %.	[36]
Glasses containing lead borate and doped with samarium and gadolinium for luminescent applications	Increase	increase	Increase	Refractive index, molar refraction, and polarizability were found to increase in proportion to increased Sm_2O_3 and Gd_2O_3 content, indicating that the glass samples exhibit visible spectrum emission	[25]

The role of rare-earth ions (REIs) as network modifiers explains these structural changes in the glass. By introducing symmetric non-bridging oxygen (NBO) ions and disrupting the bonds of asymmetric bridging oxygen, REIs integrate into the glass network. This incorporation leads to a restructuring of the glass network's internal structure, resulting in a reduced bandgap energy, an increased refractive index, and a higher degree of disorder along with an increased content of defect states within the glass network.

Physical features of REI doped glasses

Erbium (Er^{3+}) ion doped glasses

Glasses can be significantly altered in their physical properties by erbium ion (Er^{3+}) doping. The concentration of $Er^{3+,}$ the host glass matrix, and the intended applications all influence the degree of these effects occur. According to research, the density of some particular glasses increases when the concentration of Er^{3+} increases [60-62]. The presence of Er^{3+}, which is heavier than other substances, causes this phenomenon, which could be the cause of an increase in density. The quantity of Er3+ ions in the glass matrix increases with the molar volume [31-33]. Because REI forms NBO, incorporating it into a glass matrix could increase the molar volume [37,63] and also loose-packed structure because REI breaks down the bonds. Other physical features such as r_p, r_i, f_s, dielectric constant, and metallization criterion could also affect the physical features of glass samples. The decrease of r_p and r_i in borotellurite (BTBME), tellurite glass (ET) and phosphate (PKEr) glass with an increase in Er3+ content improves the polarizability and compactness of glasses in the glass network [60-62], which may result in better electrical conductivity as reported by [27,60]. Glasses doped with erbium ions can be used to measure the polaron radius and interionic distance to accomplish this. The Glass structure seems to be more compact as a result. However, when the concentration of Er^{3+} increases, the field strength does as well. The average separation between Er and Oxygen diminished because of the Er^{3+} ions' adjustment, strengthening the Erbium-Oxygen bond. In other words, a robust field is generated around erbium ions, and the strong bond that forms between Er and O adds to the increased field strength around Er^{3+}(63), which causes a decrease in r_p and r_i (60).

Nazrin *et al.* [34] investigated the optical properties of erbium-doped cadmium lithium gadolinium silicate glass, reporting that both the direct and indirect band gaps decrease with increasing molar concentrations of erbium ions. This behavior is consistent with findings in phosphate glasses (PBE) [64], barium lithium fluoroborate glasses (BLFB) [39], lithium magnesium borate glasses (LMB) [65], and silicophosphate glasses (SiPEr) [63]. The decrease in band gaps can be attributed to structural changes induced by the addition of Er_2O_3, which likely increases the number of non-bridging oxygens (NBOs) in the glass network, leading to greater structural disorder.

The presence of bridging oxygen (BO) ions, which connect structural units in the glass, is disrupted by the addition of Er_2O_3, resulting in the formation of NBOs. Bouabdali *et al.* [63] suggested that this disruption decreases the average bond energy of the glass system, contributing to reduced band gaps. However, this observation contrasts with reports for cadmium lithium gadolinium silicate glasses (CLGS) Shaaban *et al.* [1], silica borotellurite glasses (SBT) Aliyu *et al.* [47], zinc borosilicate glasses (ZBS) Razali *et al.* [36], and additional CLGS studies El-Maaref *et al.* [49], where increasing Er_2O_3 content led to higher band gaps. Increases in Er_2O_3 content have been linked to changes in the glass network that result in increased BOs and, consequently, increased band gap values. This structural modification reduces the bond length and molar volume, while also generating more BOs and decreasing NBOs [47,49]. In some glass matrices, increasing Er^{3+} content has been associated with reduced Urbach energy (ΔE), indicating decreased structural disorder [39,47]. Conversely, in SiPEr, ZT, LMB, and ZBS glasses, increased ΔE suggests higher disorder, potentially due to structural defects. The optical packing density (OPD) generally increases with higher Er^{3+} concentrations, suggesting a smaller glass matrix and increased growth of BOs,

which reduces free electrons in the system. Halima *et al.* [27] describe electronic polarizability as the strength of an electron's response to an electric field, while molar refraction measures the total polarizability of a mole of material. Research indicates that with higher dopant concentrations, both electronic polarizability and molar refraction decrease, attributed to the greater polarization potential of NBO compared to BO [1].

The incorporation of Er^{3+} into glass matrices, such as zinc tellurite [34], barium lithium fluoroborate glass (BLFBEr) Mariselvam *et al.* [39], and SiPEr Bouabdalli *et al.* [63], leads to an increase in the refractive index. This effect is due to Er^{3+} acting as a network modifier, which promotes the formation of non-bridging oxygens (NBOs) at the expense of bridging oxygens (BOs). The higher polarity of Er^{3+} facilitates the breaking of BOs and enhances the formation of NBOs, which are more polarizable than BOs. Consequently, this increases both the refractive index and the polarizability of the glass. Thus, the observed increase in refractive index and polarizability is a direct result of the greater polarizability of NBOs compared to BOs [36,59].

Samarium (Sm^{3+}) ion doped glasses

The addition of single-doped samarium ions (Sm^{3+}) can significantly alter the physical properties of glass. Research by Asyikin *et al.* [66], Shwetha *et al.* [67], and Mohan *et al.* [68] has shown that increasing Sm^{3+} content leads to higher glass density. This is likely due to the incorporation of denser samarium ions replacing lighter elements in the glass composition. Additionally, the molar volume of Sm^{3+}-doped glasses tends to decrease with increasing Sm^{3+} concentration. This decrease in molar volume, which is inversely related to density, suggests a more compact glass structure with greater network connectivity.

The reduction in molar volume indicates an increase in non-bridging oxygen (NBO) atoms and an expansion of the glass network due to doping. Sm^{3+} ions likely occupy interstitial sites in the glass network, leading to decreased free volume and a more compact structure [69]. Moreover, formulas analyzing field strength (Fs), polarizability (rp), and refractive index (ri) reveal that as Sm^{3+} concentration increases, both rp and ri decrease, signifying stronger Sm-O bonds and enhanced field strength around Sm^{3+} ions [66].

In terms of optical properties, Asyikin *et al.* [66] and Shwetha *et al.* [67] observed that the indirect optical band gap decreases with increasing Sm^{3+} concentration. This trend is attributed to the role of Sm_2O_3 as a network modifier, which can break existing glass network bonds and create NBOs. The formation of NBOs, which have less tightly bound electrons, results in a shift of the absorption band to longer wavelengths, thereby lowering the band gap energy. Thus, the internal structure and chemical composition of Sm^{3+}-doped glasses significantly influence their optical band gaps.

Erbium/Ytterbium (Er^{3+}/Yb^{3+}) ion Co-doped glasses

REIs are frequently co-doped into glasses to modify their physical properties, leading to numerous applications in areas such as materials science, electronics, and optics. The charge and size of REIs can impact the packing density and configuration of the glass network, impacting physical properties like density and thermal expansion. They also affect the glass network structure by acting as network formers

or modifiers, altering the connectivity of the glass matrix and affecting properties like viscosity and chemical durability. Density is a significant parameter that can be used to investigate changes in the glass network's geometrical configurations, level of structural compactness alterations, the coordination number of the glass-former ions, and measurements [4]. Glasses co-doped REI, like Er^{3+}-Yb^{3+} co-doped bismuth borophosphate (EBiBPxY) Naseer and Marimuhu [4], borosilicate Hassib *et al.* [30] and phosphate glasses Zhao *et al.* [70], show an increase in densities and molar volume as Yb^{3+} increases, suggesting that nBOs have been formed in the glass structure. The formation of nBOs may also be influenced by the addition of Bi_2O_3, according to Naseer and Marimuthu's [4] investigation on the impact of Er/Yb co-doping on the spectroscopic performance of bismuth boro-phosphate glasses for photonic applications. An additional explanation for this increase might be the Yb^{3+} ions' large ionic radius, which causes them to occupy interstitial voids and enlarge the glass network [30].

Co-doping glass samples with erbium (Er) and ytterbium (Yb) ions can greatly affect their optical properties, including refractive index, band gap, and polarizability. Co-doped Er^{3+}/Yb^{3+} was incorporated in borosilicate glasses in a study by Hassib *et al.* [30] As Yb^{3+} concentration increases, the band gap decreases, resulting in structural changes. The decrease is brought about by the formation of more NBOs. The same trend was reported by [4]. A glass sample's defects and disorderliness may be examined using the ΔE evaluation. In glasses with EBiBP Naseer and Marimuthu [4], the ΔE increases with an increase in the Yb^{3+} concentration in the sample matrix. This indicates that NBO will be enhanced, causing the band energies to shift to the lower energy side and subsequently lowering the energy gap and increasing Urbach energy values. The refractive index is also a critical factor in determining radiative parameters and Judd-Ofelt parameters, as well as one of the significant factors in assessing whether a material is suitable for the intended application. In addition to being linearly proportional to density, the refractive index increases as Yb^{3+} concentration increases.

Study plan for efficient laser materials

A laser operates based on the principle of stimulated emission for light amplification. When light or electrical current is introduced to an optical material such as crystal, glass, or gas, the energy is absorbed by the electrons in the atoms, causing them to move from a lower-energy orbit to a higher-energy one. This process of stimulated emission amplifies the light signal. Lasers utilize the quantum properties of atoms to emit and absorb photons-tiny particles of light. Atoms can be stimulated by light or another energy source, including other lasers, to return their electrons to their ground state, releasing more photons in the process. The efficiency of photon generation at a specific wavelength depends on the energy level structure of the ions within the material being amplified. In innovative optical devices like glasses, rare earth ions (REIs) often have optimal energy level structures that can operate at various pumping wavelengths [9]. To understand the quantitative optical properties of REIs in glasses, it's essential to assess both radiative and non-radiative decay processes of the relevant 4*f* levels [49,59]. The Judd-Ofelt (J-O) theory, established in 1962, describes the strength of electron transitions within the 4*f* shell of REIs when electromagnetic radiation is absorbed or emitted. The J-O theory provides intensity parameters (Ωλ for λ = 2, 4, and 6) that help calculate the oscillator strength (f_{cal}) of induced electric dipole transitions from the initial state (JΨ) to

the final state (J'Ψ') [71]. **Figure 6** illustrates the research plan for analyzing these transitions and their implications for the optical performance of REI-doped glasses.

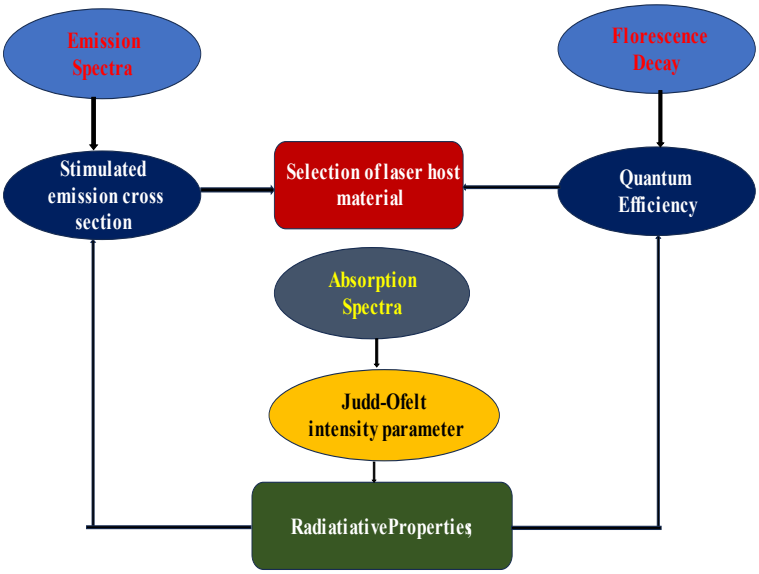

Figure 6 Study plan for efficient laser materials.

The consequence of bonding ((δ) and nephelauxetic (β) parameters in absorption spectra

Using bonding parameters and Nephelauxetic parameters, an observed absorption band site can be used to examine the type of metal-ligand bond present in a glass matrix. The type of metal-ligand bond can be predicted based on whether the value is positive or negative of bonding parameters. In the studies conducted by Deopa *et al.* [72] and his co-researchers to determine the covalency between REI and oxygen ligands using the nephelauxetic effect brought on by REIs' partially filled *f*-shells. The doped REI 4*f* electronic orbits have been distorted by the host matrix's ligand field environment. The overlap of oxygen orbits and *4f* orbits lowers the energy level structure of REI. Consequently, a change in wavelength will occur. The estimation of the nephelauxetic ratio (β) and bonding parameters (δ) can be utilized to mathematically illustrate the type of bonding that occurs between oxygen ligands and REI doped in the host matrix. The parameters are shown in **Table 5** and depend on whether the metal-ligand bond is covalent or ionic, positive or negative.

Table 5 Nephelauxetic ratio and bonding parameters in REI doped glasses between different glass hosts.

Research title	Glass system	Rare earth used	Major finding	References
Concentration-related Spectroscopic characteristics of boro	ZSBPO	Sm^{3+}	The bonding parameters were found to have a negative value, indicating that the Sm–O bond is ionic	[73]

Research title	Glass system	Rare earth used	Major finding	References
phosphate glasses doped with Sm^{3+}				
Samarium doped tellurite glass: Ligand field and Judd-Ofelt intensity parameters	TZS (Zinc Tellurite glass)	Sm^{3+}	Positive δ values are a sign of covalent bonding dominance, and it has been observed that they increase with an increase in Sm3+ concentration. NBOs increased because of a decrease in BO numbers	[74]
Structural and luminescence properties of samarium doped lead alumino borate glasses	PAB	Sm^{3+}	Covalent bonding between the Sm-O bonds was reported to be indicated by the bonding parameter's positive values.	[68]
Studies on the concentration dependence and luminescence of barium lithium fluoroborate glasses doped with erbium	BLFB	Er^{3+}	The δ values that were reported showed a positive (+) correlation with an increase in erbium ion, suggesting a covalent bond between the Er3+ ions and the ligands of the glasses	[39]
Impact of Sm^{3+} ion concentration on borosilicate glass for applications in reddish-orange luminescent devices	ZnBiSrBSi (Borosilicate glass)	Sm^{3+}	The bonding parameter's negative values have revealed the ionic character of the bonding between Sm3+ ions and the ligands surrounding them, which reduces as the concentration of REI increases.	[72]
The bio-silicate borotellurite glass system doped with erbium oxide: Physical properties, ligand field, and Judd-Ofelt intensity parameters	bio-silicate borotellurite (BSBT)	Er^{3+}	The bonding parameters' positive (+) value demonstrates the glass matrix's covalent nature.	[37]

Research title	Glass system	Rare earth used	Major finding	References
Glasses for optoelectronic devices; orange color emitting Sm^{3+}-doped borosilicate	LPZABS	Sm^{3+}	The reported negative values for δ suggest that Sm^{3+} ions form bonds with surrounding ligands. The total increase in δ value (toward the positive side of a scale) with Sm^{3+} ion content suggests that the ionic character between Sm^{3+} ions and oxygen ligands in the titled glasses decreasing	[69]

Parameters of the ligand field (racah and crystal field strength parameters)

The crystal field strength and Racah parameters, known as ligand field parameters, can be derived from the lower wavelength absorption spectra using the values for V_1, V_2, and V_3. Hamza *et al*. [53] reported on the Racah parameters (R and C) and crystal field strength for Er^{3+}-doped BSBT (bio-silicate borotellurite) glasses. Their findings indicate that the Racah parameters decrease with increasing Er^{3+} concentration, suggesting that the environment around Er^{3+} becomes more covalent. This reduction in Racah parameters is attributed to the diminished electron-electron repulsion within the d-orbital of the metal ion, which also results in a larger orbital size for the complex.

Additionally, the crystal field strength increased with higher concentrations of Er^{3+}. Tanko *et al.* [74] observed similar trends with Sm^{3+} ions, where increasing Sm^{3+} concentration led to a decrease in Racah parameters (R and C), reflecting the covalent nature of Sm^{3+} bonding with the ligand environment. The Nephelauxetic ratio (h) increased with Sm^{3+} content, indicating enhanced covalency in the Sm^{3+}-ligand bond. Concurrently, the crystal field parameters (Dq and Dq/B) increased, suggesting a stronger crystal field strength in the samples.

Judd-Ofelt (J-O) analysis and oscillator strengths

To explain the peaks, Judd and Ofelt proposed a theory and determined the J-O intensity parameters, Ω_λ (λ = 2,4,6). J-O intensity characteristics in terms of Ω_λ (λ = 2, 4, and 6) are crucial for assessing the effectiveness of laser and luminescent materials. Theoretical and experimental transition oscillator strengths of multiple excited multiplets were assessed to determine the 3 J-O intensity parameters, which were then minimized using least-squares or chi-square techniques [75]. These variables are connected to other features of the host glass system, including the covalency of the RE-O bond and the crystal field symmetry at the REI site. Short-range coordination effects are generally associated with the Ω_2 parameter. A larger Ω_2 value is expected due to the asymmetry of the RE ligands and increased polarization. When the oscillator strength of the hypersensitive transition is relatively high, Ω_2 has a higher value. The highest value of Ω_2 in the glass system indicates slightly reduced asymmetry and increased covalency, making the hypersensitive transitions and the local structure of the rare earth ions (REIs) more significant for the Ω2 parameter

compared to other Judd-Ofelt intensity parameters [54,76,77]. This finding is consistent with the bonding nature estimate provided by the nephelauxetic effect [37,39]. In some glasses, the Ω2 intensity parameter is found to be greater than Ω4 and Ω6 values, suggesting that the local environment around the REI site is highly asymmetric and disordered, with a high degree of covalency between the ligand bonds and the REI site. The Ωλ calculations offer essential insights into the glass configuration and the rate of change in RE energy levels. In contrast, Ω4 and Ω6 parameters are influenced by long-range effects Tayal and Rao [69] Furthermore, they facilitate an understanding of the structural disorder surrounding REIs (Ω_2) and bulk parameters (Ω_4 and Ω_6), such as rigidity and viscosity [69]. In synthetically doped glasses, the $\Omega_{4,6}$ is less sensitive to the surrounding environment. In many cases, the spectroscopic quality ($X= \Omega_4/\Omega_6$) factor is employed to determine the laser capacity of a transition in terms of Ω_4/Ω_6 [37,54]. **Table 6** presents an evaluation of the J-O parameters obtained for various RE^{3+} doped glasses for comparative analysis

Table 6 The J-O intensity and quality factor parameters are compared for various glass hosts Ω_λ ($\lambda = 2,4,6$).

Glass samples/Reference	Ω_2 ($x10^{-20}$ cm^2)	Ω_4 ($x10^{-20}$ cm^2)	Ω_6 ($x10^{-20}$ cm^2)	Trends	$X = \Omega_4/\Omega_6$
Bio-silicate borotellurite glass (BSBT) [37]	4.179	1.943	1.059	$\Omega_2 > \Omega_4 > \Omega_6$	1.83
Erbium-doped cadmium lithium gadolinium silicate glasses (CLGS) [49]	0.786	0.987	0.373	$\Omega_2 > \Omega_4 > \Omega_6$	2.646
Erbium-doped phosphate glass (PBEr) [64]	5.64	2.38	1.55	$\Omega_2 > \Omega_4 > \Omega_6$	1.69
Samarium doped Lithium lead zinc alumino borosilicate (LPZABS) glass [69]	1.49	2.38	1.36	$\Omega_6 > \Omega_4 > \Omega_2$	-
Cadmium lithium gadolinium silicate glass (CdLiGdSi) [1]	8.49	7.86	1.25	$\Omega_2 > \Omega_4 > \Omega_6$	-
Erbium-doped gadolinium-calcium silica borate glasses (BSGdCa:Er) [54]	3.16	1.32	0.99	$\Omega_2 > \Omega_4 > \Omega_6$	1.33
Oxyfluoride aluminosilicate glass (EBiBP) [76]	4.847	0.771	1.25	$\Omega_2 > \Omega_6 > \Omega_4$	-
[73]	0.25	3.60	3.15	$\Omega_4 > \Omega_6 > \Omega_2$	1.14

Glass samples/Reference	Ω_2 (x10^{-20} cm^2)	Ω_4 (x10^{-20} cm^2)	Ω_6 (x10^{-20} cm^2)	Trends	X = Ω_4/Ω_6
BSiAlZnLi0.5Yb^{3+} [30]	0.230	0.123	0.196	$\Omega_2 > \Omega_6 > \Omega_4$	0.62
Erbium-doped barium lithium fluoroborate (BLFB) [39]	3.74	0.96	1.70	$\Omega_2 > \Omega_6 > \Omega_4$	0.56
Lithium sodium (LSG) borosilicate [78]	1.59	0.61	0.15	$\Omega_2 > \Omega_4 > \Omega_6$	-
Er^{3+}-Yb^{3+} co-doped bismuth bororphosphate glass (EBiBP) [4]	3.994	1.288	1.158	$\Omega_2 > \Omega_4 > \Omega_6$	1.19
Structural and optical studies of Sm^{3+} ions doped niobium borotellurite glasses (TSZNB) [79]	5.21	7.85	3.70	$\Omega_4 > \Omega_2 > \Omega_6$	2.12

The magnitude of Ω_4, which is greater than Ω_6 and Ω_2, in samarium doped-boro phosphate glass suggests the crystal field of REI deviates from cubic symmetry and suggests the glass is more rigid [9]. The borotellurite glass (TSZNP) J-O parameters trends $\Omega_4 > \Omega_2 > \Omega_6$ were not conformed with other glasses in **Table 6**, the glass matrices become less rigid and viscous in the same sequence as the Ω_6 parameter decreases when modifier ions are incorporated, which is Mg→ Ca→ Sr [79].

Table 6 highlights how the potential of the host materials for laser operation of a given transition in a REI is evaluated in terms of Ω_4 and Ω_6 Hraiech *et al.* [64] using the spectroscopic quality factor, which is given by (Ω_4/Ω_6). A higher laser transition is indicated by a lower spectroscopic quality factor value. This is due to REI-doped glass exhibiting a more intense laser transition with a lower quality factor value [37]. The glasses' optical quality and stimulated emission are determined by their spectroscopic quality factor (Ω_4/Ω_6). The increased calculated values ($\Omega_4/\Omega6$) of the examined REI doped glasses show that they have outstanding optical quality and are suitable for use in photonic applications. Vijayakumar and Marimuthu [73], laser host medium Asyikin *et al.* [68] and predict efficient stimulation emission [80].

The intensity of absorption peaks for rare earth ion (REI) *f-f* transitions in doped glasses is predominantly influenced by the oscillator strengths (f). These can be determined for various glass systems using Judd-Ofelt (J-O) analysis. The J-O theory allows for the calculation of the theoretical oscillator strength (f_{cal}) for electric dipole transitions between the ground state (ΨJ) and excited states (Ψ'J') within the 4*f* configuration. The least-squares fit method is employed to achieve the best match between experimental and calculated oscillator strengths. Oscillator strength is a critical parameter for assessing the strength of *f-f* transitions in the absorption spectra of doped glasses [73]. Experimental oscillator strengths can be derived from the area under the absorption bands. J-O parameters $\Omega\lambda$ (λ = 2, 4, and 6) are computed using results obtained in conjunction with oscillator strengths calculated through doubly reduced matrix

elements and the least-squares fitting approach [9]. A small root means square (rms) deviation between experimental (f_{exp}) and calculated (f_{cal}) oscillator strengths indicate a good fit, consistent with J-O theory [31,81]. The rms deviation measures the accuracy of the fit between experimental and theoretical oscillator strengths. **Table 7** shows the positions of the peaks, the bands assigned to them, and the experimental and calculated oscillator strengths for a few glasses.

Table 7 Calculated and experimental oscillator strengths of selected REI-doped glasses; TRZNB Ravi *et al*. [79], PAB Mohan *et al.* [68], LCZSFB Reddy *et al.* [9] and LBGS [31].

Experimental	**TRZNB**		**PAB**		**LCZSFB** (C. M.)		**LBGS**	
Transition $^6H_{5/2}\rightarrow$	f_{exp}	f_{cal}	f_{exp}	f_{cal}	f_{exp}	f_{cal}	f_{exp}	f_{cal}
	1.091	2.030	0.25	4.968	0.57	1.03	0.29	0.21
$^6F_{1/2}$	4.550	4.040	0.361	8.320	1.74	0.04	1.50	1.40
$^6H_{15/2}$	5.340	5.110	1.623	4.932	3.74	3.01	2.52	2.62
$^6F_{3/2}$	3.740	7.431	1.439	4.366	4.77	5.08	2.17	2.41
$^6F_{5/2}$	4.360	7.780	3.012	1.086	7.32	7.53	2.21	1.62
$^6F_{7/2}$	5.166	4.960	2.987	1.412	4.97	4.78	1.41	0.01
$^6F_{9/2}$	0.392	0.73	5.249		1.26	0.76	0.38	0.75
$^6F_{11/2}$								
	$\delta_{rms} = \pm 0.45\times10^{-6}$		$\delta_{rms} = \pm 0.281\times10^{-6}$		$\delta_{rms} = \pm 0.76\times10^{-6}$		$\delta_{rm} = \pm 0.53\times10^{-6}$	

In glasses doped with samarium ions, such as TRZNB (borotellurite), PAB (lead alumino borate), and LCZSFB (lead calcium zinc sodium fluoroborate), the absorption bands show stronger oscillator strengths. This enhancement in oscillator strengths can be attributed to the higher value of the asymmetric component of the electric field produced by the ligand environment surrounding the Sm^{3+} ion. The luminescence of the glass, which results from the relaxation of excited electrons back to their ground state, is influenced by the type of REIs and the local electronic environment at the REI site.

Radiative and luminescence properties of REIs glass doped

Furthermore, to understand the REIs luminescence of a glass, radiative properties such as branching ratio (β_R), stimulated emission cross section (σ_{emi}), radiative lifetime (τ_{Rad}) and radiative transition probabilities (A_R) parameter for different emission intensities must be evaluated using the J-O theory. An important factor in discovering the lasing power of emissive transitions is the branching ratio (β_R) [39]. The possibility of achieving stimulated emission under appropriate excitation conditions is partially characterized by the branching ratio, which is vital. It has been established that there is a greater possibility of laser emission in an emission transition with a β_R of greater than 50 %. **Tables 8** provide the following conclusion: Its suitability for laser action and optical communication applications [31] is shown by the calculated β_R value for LPZABS Tayal and Rao [69], LCZSFB Reddy *et al.* [9], PAB Mohan *et al.* [68], ZSBP Vijayakumar and K Marimuthu [73], and LBGS Khan *et al.* [31] glasses being greater than 0.5.

Table 8 effective linewidth, $\Delta\lambda_p$ (nm), transition probability, A (s^{-1}), peak wavelength, λp (nm), experimental and calculated branching ratios (β_R), gain bandwidth ($\sigma_{emi}\times\Delta_{\lambda p}$) stimulated emission cross-section, σ_{emi} ($\times 10^{-22}$ cm^2) and optical gain ($\sigma_{emi} \times\tau_R$) of REI doped with different glass host.

Glass sample	$\boldsymbol{\lambda_p}$	$\boldsymbol{\Delta\lambda_p}$	$\boldsymbol{A_R}$	$\boldsymbol{\sigma_{emi}}$	$\boldsymbol{\sigma_{emi}\times\Delta\lambda_p}$	$\boldsymbol{\sigma_{emi}\times\tau_R}$	$\boldsymbol{\beta R}$	
							exp	***cal***
LPZABS [69]	598	11.30	163.34	3.83	23.50	4.34	0.4856	0.395
LCZSFB [9]	602	14.49	264.88	12.60	18.3	11.85	0.44	0.590
LBGS [31]	600	-	106.90	2.68	-	9.49	0.53	0.390
ZSPB [73]	598	10.61	146.25	9.068	86.35	16.28	0.501	0.505

The glass is appropriate for laser applications if its value of β_R is larger i.e greater than 50 %, as this indicates a higher emission cross-section [9,30,76]. Naseer & Marimuthu [4] state that, For EBiBP glasses, the stimulated emission cross-section is maximum for the $^4S_{3/2} \rightarrow {}^4I_{15/2}$ transition, which is necessary to achieve low-threshold and high-gain lasering operation. For photonic applications like green light-emitting lasers, the use of boro phosphate glass-matrix is thus advised. A crucial factor in determining the materials' quantum efficiency and possible laser performance is the stimulated emission cross section (σ_{emi}), which demonstrates the rate at which energy is taken out of the laser material. The changes will affect the host-matrix composition. The large, stimulated emission cross-sections are useful characteristics for high gain, low threshold laser applications, which are utilized to attain continuous wave laser CW action. The absorption cross-section can also be used to compute the stimulated emission cross-section using the McCumber theory. In a study on stimulated emission cross-section, Basavapoornima *et al.* [82] evaluated the possibility of a laser effect by applying McCumber's theory. and the outcomes showed that the absorption and emission cross-sections first rise before declining as the Yb^{3+} ion concentration rises. The variation results from reabsorption caused by the spectral overlap of emission and absorption of Er^{3+} ions [12,83]. Kesavulu *et al.* [54] study on the impact of Er^{3+} ions on the optical and photoluminescence characteristics of glasses. Additionally, it was suggested that the McCumber theory provides a useful method to evaluate the stimulated emission cross-section of the Er^{3+} ion's $^4I_{13/2}$–$^4I_{15/2}$ transition based on the measurement of the absorption spectra. A broadband amplifier needs a larger emission cross section since the optical materials demand a high rate of energy extraction. This may correspond to the $^4I_{13/2}$-$^4I_{15/2}$ manifold's increased line strength value. Furthermore, an increase in the concentration of Er^{3+} has a significant effect on the emission cross-section. For lasers and optical amplifiers to operate as well as feasible, the emission cross-section must be increased to its maximum level [82]. As stated earlier, the surrounding host matrix in which a trivalent rare-earth ion is integrated has a major effect on the characteristics of the stimulated emission of the ions [76].

In assessing laser performance, the gain value is an additional crucial factor. The optical gain additionally impacts how efficient the medium containing the REI will be in amplifying information. Diagnostics, optical data storage, color displays, and underwater communication all depend on high-gain laser applications. A high gain application is an essential property for lasers to generate continuous wave (CW) laser action since it increases with stimulated emission cross section (σ_{emi}) at a lower threshold value,

along with the β_R [69,79]. A population inversion of more than 40 % results in positive gains. The study sample is covered by this range of wavelengths with a flat gain bandwidth that spans the S-band (1460 - 1530 nm) and C-band (1530 - 1565 nm) in the optical communication window. Thus, nominal inversion would be a simple way to amplify up the S + C-band. [54]. High-gain laser applications are expected to have a relatively large, stimulated emission cross-section. Effective optoelectronic device fabrication is highly dependent on the optical gain ($\sigma_{emi} \times \tau_R$) and gain bandwidth ($\sigma_{emi} \times \Delta\lambda_p$) parameters. According to **Table 8**, Indications point to LCZSFB, LiBiAlBSi and ZSPB as potential candidates for laser application due to the higher value of σ_{emi} in the transitional state $^4D_{5/2} \rightarrow {}^6H_{7/2}$. Consequently, the result revealed the optimum for luminescent applications as a possible active medium in solid-state lasers. in the visible orange region [69,73,79]. In conclusion, glass with greater values of the stimulated emission cross-section and branching ratio may be utilized for high-gain laser purposes. Medical diagnostics, underwater communication, color displays, and optical data storage are some of these applications [12,83].

Bandwidth ($\Delta\lambda_{eff}$) is another crucial aspect of the wavelength division multiplexing network (WDM)-powered REI integrated optical amplifier (Erbium-Doped Fiber Amplifier, or EDFA) optical communication system. higher A_T, β_R, σ_{emi} and gain bandwidth values in the glass transition indicate that it may be a suitable active medium for reddish-orange emission in solid-state lasers [73]. In Naseer and Marimuthu [4] investigation of EBiBP's spectroscopic performance for photonic applications. It was reported that for each produced sample, the $\Delta\lambda_{eff}$ values vary greatly with higher Yb^{3+} concentration. This suggests that increasing the amount of ytterbium ion in the surrounding network affects the ligand fields around the Er^{3+} position, which subsequently causes the luminescence band in the emission spectra to broaden. The surroundings of the luminescent Er^{3+} and Yb^{3+} ions (i.e co-doping) may be ascertained by examining the lifetime of excited states using single and non-exponential fitting techniques. The optical amplifier performance has a direct relationship with 2 important parameters in the spectroscopic study: the quantum efficiency for the $^4I_{13/2} \rightarrow {}^4I_{15/2}$ transition, as demonstrated by the Er^{3+}-Yb^{3+} co-doped systems, and the $^4I_{13/2}$ level lifetime. Yb^{3+}-Er^{3+} ion (co-doped) energy transfer efficiency can be evaluated using the Burshtein theory. Consideration is given to the impact of energy movement between sensitizing ions in the Burshtein model. Presumably, energy moves between Yb^{3+} sensitizers until it comes across an Er^{3+} activator ion. Given that ytterbium (sensitizer) and Er^{3+} (activator ion) are in small concentrations and theoretical approach was chosen [12]. In Nasser *et al.* [83] study on PTR glasses, it was found that the majority of the ytterbium ion absorption in the glasses was caused by a 980 nm laser line excitation due to their large absorption cross-section of about 1 μm. Put differently, Eq. (9) indicates that an effective and indirect pump of erbium ions is produced by the 980 nm laser excitation.

$$^2F_{5/2}[Yb^{3+}] + {}^4I_{15/2}[Er^{3+}] \rightarrow {}^2F_{7/2}[Yb^{3+}] + {}^4I_{11/2}[Er^{3+}] \quad (9)$$

It was found in the study that when Yb_2O_3-co-doped glasses were also increased, respectively, ytterbium to erbium ions in erbium had a higher energy transfer efficiency. Presumably, energy moves between Yb^{3+} sensitizers until it comes across an Er^{3+} activator ion. A larger up-conversion luminescence is produced when Yb^{3+} levels rise because energy loss is considerably decreased and the transfer of Yb^{3+} to

Er^{3+} energy becomes simpler. Subsequently, the intensity of luminescence may decrease above 0.5 weight percent Yb^{3+}, possibly due to increased reverse-energy transfer between the REI. Basavapoornima *et al.* [82] and Naseer and Marimuthu [4] have suggested that the strong up-conversion luminescence of glasses could be advantageous for fortifying up-conversion optical devices and amplifiers. For some of the glasses under study, it is discovered that the transfer efficiencies rise as Yb^{3+} does. Transfer efficiencies, which can approach 60 %, are largely dependent on the corresponding concentrations of the donor and activator ions. The fact that as energy transfer efficiency increases, the lifetimes of the sensitizer (Yb^{3+} ions) and activator (Er^{3+} ions) decrease respectively [12,70,82] validates the theory that energy is transferred from Yb^{3+} ions to Er3+ ions

PL decay analysis

Excited decay state

A deeper understanding of the excitation mechanisms of rare earth ions (REIs) can be achieved by examining their intra-4f electron transitions. Excess energy absorbed by an REI can be transferred to a neighboring REI or result in combined relaxation processes, allowing the excited REI to return to its ground state through radiative transitions or phonon emission. An excited REI may de-excite itself either radiatively, by emitting phonons through a nearby REI, or via combined relaxation methods. At very low dopant concentrations, where interactions between optically active REIs are minimal, fluorescence decay curves often fit a single exponential function. The first e-folding times in such cases can be used to determine the lifetime of the excited level, indicating that energy transfer between luminescent ions is not significant. However, as REI concentration increases, the typical decay time of the glasses decreases. This reduction is attributed to non-radiative energy transfer mechanisms, such as cross-relaxation, where energy is transferred from an excited donor ion to a ground-state acceptor ion [73]. The Judd-Ofelt (J-O) theory can be used to determine the experimental lifetime (τm) of REI-doped glasses. Studies have shown that the experimental lifetime is substantially shorter than the predicted lifetime (τ_R) and decreases as REI concentration increases. This decrease is often due to multi-phonon non-radiative decay or efficient energy transfer between REIs via cross-relaxation [31].

The energy transfer by multiphonon relaxation is essentially negligible since the energy difference between the $^4G_{5/2}$ level and the subsequent level is significantly higher than the phonon energy of the host [73]. Thus, the primary means by which energy is transferred between REI is through the cross-relaxation mechanism [68]. In REI-doped glasses, cross-relaxation between 2 nearby REI occurs when their absorption and emission energy levels are equally spaced. Acceptor ions in the ground state undergo cross-relaxation and enter the metastable state when they receive energy from donor ions in the more excited state. Ultimately, the ground state of the donor and acceptor ions is restored through non-radiative decay. The fact that all of the chosen glasses have reported higher energy transfer (E_T) rates is responsible for the significant discrepancy between the calculated and experimental lifetime values. In line with *Deepa et al.* [53], a decrease in the τ_{exp} values of the $^4F_{3/2}$ emission level may occur with an increase in REI concentrations due to energy transfer through non-radiative decay rates (W_{NR}) at high concentrations. This finding applies to the glasses that are the subject of the study.

Quantum efficiency (η), the standard term for the ratio of a luminescent material's emitted to absorbed light intensity, is another crucial factor for determining a luminescent material's efficiency. It is a proportion of photons that are emitted to those that are absorbed [84]. quantum efficiency (η) measures the ratio of emitted photons to absorbed photons. It is influenced by various factors, including the emission cross-sections, radiative transition probabilities, lifetimes of metastable states, the concentration of REIs, and the ligand field effects [79]. The high-value quantum efficiency (η) of REI-doped glasses were reported for LPZABS, BLFBEu Mariselvam *et al.* [59], BSKNLNd Deepa *et al.* [53], LCZSFB, LBGS, PAB and TRZNB. **Table 9** represents the decay properties of different glass hosts. This proves the effective lasing action in the visible orange region (donor and acceptor ions) was achieved by the selected glasses, not by the calculated values of the ZSBP glass samples, which were found to decrease as the concentration of the Sm^{3+} ions increased owing to the efficient energy transfer between the Sm^{3+} ions Tayal and Rao [69] to transfer energy through cross-relaxation. Additionally, it was noted that the PL decay curves for LPZABS glasses nearly showed a single exponential decay when they were excited at 400 nm. This is because the developed glass structure had better quantum efficiency values, making it suitable for use in broadband amplifier applications [4]. and an excellent option for laser emission as well [53].

Table 9 Comparison of decay properties, quantum efficiency η (%), lifetime (experimental (τ_R) and calculated ($\tau_{cal)}$ (ms) for selected glasses doped with REI.

ZSBP		**LBGS**		**LPZAB**		**BLFBEu**		**BSKNLNd**	
τ_R	τ_{cal}	τ_R	τ_{cal}	τ_R	τ_{cal}	τ_R	τ_{cal}	τ_R	τ_{cal}
1.990	4.103	2.468	-	6.122	2.850	1.92	2.07	2.28	2.44
1.821	3.103	1.663	-	4.592	2.360	2.57	2.06	2.13	2.44
1.511	3.362	1.099	-	3.002	2.198	2.49	2.05	1.88	2.44
1.001	3.062	0.756	-	2.736	1.460	2.39	2.04	1.31	2.44
0.403	1.819	0.566	-	2.564	1.250	2.30	1.95	-	-
η (%) = 49.00		η (%) = 46.00		η (%) = 73.21		η (%) = 85.00		η (%) = 93.0	

Finally, the donor and acceptor ions are returned to their ground state via non-radiative decay. The significant discrepancy between the calculated and experimental lifetime values is what creates the in crease in energy transfer rate, based on the results of the rate of energy transfer during cross-relaxation (WET). Quantum efficiency is further reduced by the cross-relaxation energy transfer between the donors (excited Sm^{3+} ions) and acceptors (ground state Sm^{3+} ions).

Non-radiative relaxation

A non-radiative process enables an excited rare earth ion (REI) to relax to a lower energy state after photon absorption. In cases where only a single local environment is present and the excitation source is removed, deviations from a single exponential decay can indicate non-radiative decay due to energy transfer within the 4*f* electron system. Energy transfer between identical RE^{3+} ions typically involves excitation migration and cross-relaxation, while transfer within the same ion may occur between different multiplets with varying energy levels. The measured lifetime (τm) of the emitting state is given by the reciprocal of the total decay rate (1/τm), which is the sum of the radiative (AR) and non-radiative (WNR) decay rates.

Color chromaticity coordinates

White light-emitting diodes (w-LEDs) are a key element in solid-state lighting, surpassing traditional incandescent and fluorescent lamps in several areas, including energy efficiency, brightness, longevity, compactness, and performance in low temperatures. Rare earth ion (REI)-doped glasses are especially advantageous for blue LEDs with yellow phosphor coatings, thanks to their cost-effectiveness, consistent emission, ease of manufacturing, and excellent thermal stability [85]. A spectrophotometric method of evaluating the photoluminescence emission spectra can be employed with the CIE 1931 (Commission International d'Eclairage) coordinate system. To demonstrate every possible color, this global chromaticity diagram combines the 3 primary colors [31,59,85,86]. The emission color of any light source can be described by 3 dimensionless quantities called color-matching functions, x(λ), y(λ), and z(λ) [87].

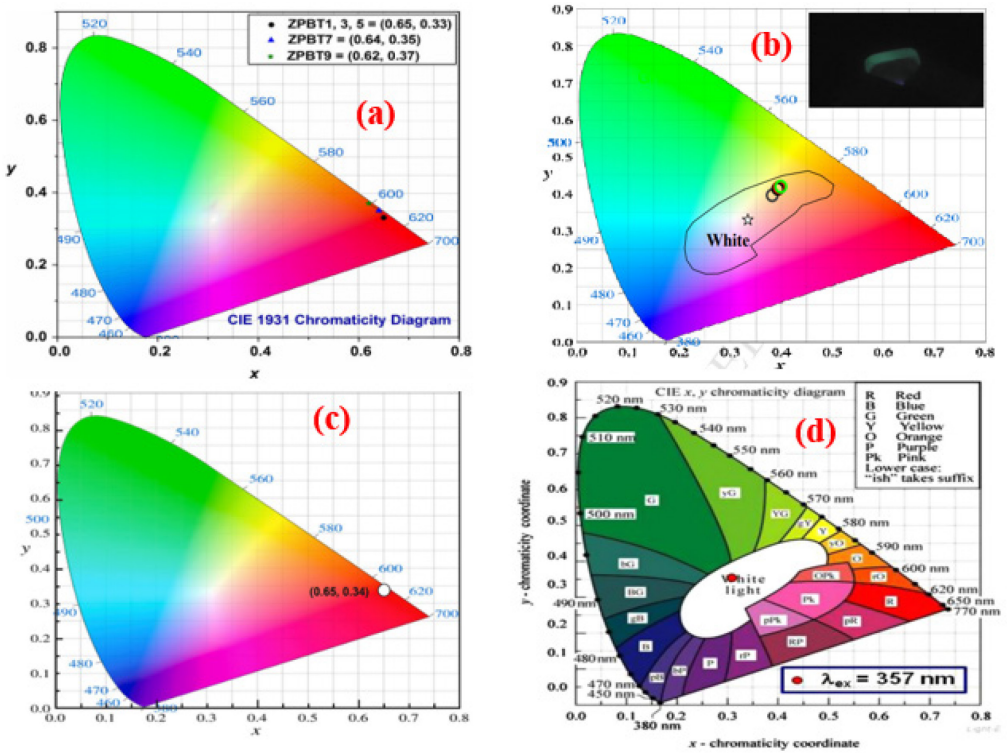

Figure 7 Diagram of CIE 1931 for (a) Eu^{3+}-ZPBTD Borges *et al.* [88], (b) DY^{3+} doped borophosphate glasses. Jha and Jayasimhadri [87], (C) Eu^{3+}-BLFB Mariselvam *et al.* [59] and (d) DY^{3+}-ZnAlBiB [40].

The CIE 1931 chromaticity diagram of the different glasses under study is depicted in **Figure 7**, and it is stated that the glasses' chromaticity coordinates are found to lie in the region of white light. The standard white light emission x, y coordinates (x = 0.33, y = 0.33) are always located in the middle of the CIE 1931 chromaticity diagram. The x, y coordinates in LBGS-Sm^{3+} and LSBPDY^{3+} are closer to the standard equal energy points, indicating that the glasses are appropriate for white light emitting sources [31,87]. The Y/B ratio values can be modified to adjust the emission color of the 1.5DY^{3+}-ZnAlBiB glasses. Glass sample with 1.5Dy3+ concentration can be used to create an efficient white light-emitting diode at a wavelength of 357nm according to Swapna *et al.* [41]. The LBGS-Sm^{3+} glass's measured color coordinates fell within the orange region of the CIE diagram, making the glasses feasible choices for orange light-emitting devices [(31)]. The CIE diagram in **Figure 7(c)** illustrates that the glass 2.0Eu^{3+}-BLFB is also suitable for red-color laser applications and display devices [61]. When designing light-emitting diodes (LEDs) and assessing phosphor performance, key metrics to consider include the Color Rendering Index (CRI), Correlated Color Temperature (CCT), and Color Purity (CP).

The CCT, represented on the chromaticity diagram, indicates the temperature of the nearest Planckian black body locus to the LED's operational point. **Table 10** provides details on CCT values, the Y/B ratio, and CIE color coordinates. McCamy's approximation can be used to determine the CCT. Generally, a higher CCT is associated with improved visual clarity and enhanced brightness perception compared to a lower CCT. The low color purity value indicates the purity of the white light emission.

It was discovered that the lead glass sample with 5 mol % Eu^{3+} by Zagrai *et al.* [58] was appropriate for use as w-LEDs for outdoor illumination. Additionally reported to be appropriate were the CCT situated in the cool light, the low CPI and high CRI values, as indicated in **Table 10**, and the CIE coordinates in white-light emission (0.337, 0.331). Mishra *et al.* [81] recommend using a commercial BLUE/UV LED chip. Glass BBS05 under λex = 348 nm excitation is highly appropriate for producing white light, or average daylight illumination [81,82].

Table 10 Color correlated temperature (CCT, K), Y/B ratio, and chromaticity color coordinates (x, y) of some RE^{3+}-doped glasses.

Glass samples	Y/B ratio	Color coordination (x, y)		CCT (K)	References
Lithium barium gadolinium silicate glasses doped with Sm3+ for Orange LEDs	-	0.59 0.59	0.49 0.49	1721 1721	[31]
Barium lithium fluoroborate glasses doped with europium	-	0.650 0.649	0.350 0.349	-	[59]
	1.18	0.312	0.276	-	[40]

Glass samples	Y/B ratio	Color coordination (x, y)		CCT (K)	References
Zinc Alumino Bismuth Borate glasses doped with Dy3+ for use in lasing materials and white LEDs	1.18	0.373	0.394		
Glasses doped with Dy3+ for borophosphate lasers and white LEDs	1.871 1.791	0.380 0.391	0.397 0.414	4145 3986	[87]
Barium silicate glasses doped dysprosium for the emission of white light	1.12 1.13	0.31 0.31	0.34 0.34	6602 6749	[86]
Photonic applications of Eu^{3+} ions in lead glass		0.337 0.202	0.331 0.198	5289 950,000	[58]

RE-doped glasses in biomedicine

Rare earth elements (REE) are intriguing elements that are frequently utilized as a doping species to give nuclear and optical characteristics to bioactive glasses [89]. Research has indicated that lanthanum demonstrates antibacterial and cellular immunity properties. Both soft and hard tissue binding can be mediated by bioactive materials, which can also trigger a biological reaction. Implant materials for medical purposes have been created using bioglass and its derivatives. Bioglass is more biocompatible than other materials in more recent biological applications, such as bone and teeth implants for human bodies [84]. According to a study by Srigurunathan *et al.* [86], 6 distinct REI-ytterbium, Dysprosium, Terbium, Gadolinium, Europium, and Nudynium ion as well as their differences in dopant concentrations, were selected to produce a broad range of combinations. The findings confirmed that dopant concentration and size play important roles in shaping ZrO_2 crystalline phase behavior. With ytterbium, Dysprosium, Terbium, Gadolinium and Nudynium ions exhibiting T_1 or T_2 different characteristics that are probably going to create attention in magnetic resonance image (MRI) applications, the paramagnetic response of the ZrO_2 material influenced by RE is evident. Furthermore, Ytterbium and Dysprosium ion band contents add to the material's high X-ray attenuation properties. The combination of Gadolinium and Dysprosium ion exhibits superior mechanical and paramagnetic properties in addition to remarkable T_1 and T_2 contrast features for MRI; still exhibits good X-ray attenuation for computed tomography (CT) imaging. These combinations are the most studied compositions. It was determined that further research into REI-doped ZrO_2 systems for biomedical uses is possible.

Zhang *et al.* [87] demonstrated that mesoporous bioactive glass (MBG) nanospheres doped with 1 mol % rare earth (RE) ions exhibited excellent apatite mineralization ability in simulated body fluid (SBF) for 3 days. The release of doxorubicin (DOX) from these RE/MBG nanospheres can be effectively regulated by adjusting the type of doping ions and pH levels. The proliferation of osteosarcoma MG63 cells was significantly inhibited when DOX was released from the RE/MBG nanospheres. These results suggest that RE/MBG nanospheres are biocompatible and can function as a pH- and time-responsive release system, enhancing the anticancer activity of DOX while reducing its side effects. Consequently, RE/MBG nanospheres have potential as a versatile implantable carrier material for clinical bone repair and the treatment of cancerous bone defects. Ershad *et al.* [85] compared the physicomechanical properties and *in vitro* bioactivity of 45S5 bioactive glasses with varying concentrations of cerium oxide (CeO_2) and lanthanum oxide (La_2O_3). Their findings revealed that as the concentrations of La_2O_3 and CeO_2 increased, the nucleation and crystallization temperatures decreased, leading to improved microhardness and flexural strength. Structural analysis showed that the samples maintained a hydroxycarbonate (HCA) layer on their surfaces even after being immersed in SBF solution.

Although an assessment of apoptosis indicates that substituting lanthanum and cerium oxide reduced apoptosis, The improved cell proliferation and viability of bioactive glasses have been demonstrated by an *in vitro* cell culture study; consequently, the developed REI-substituted bio-glass is a good option for bone tissue engineering. The application of REIs has been the focus of numerous studies for a long time. Despite the development of many products and advancements, more research on the future application of REIs doped glasses as fiber optics can help address some of the telecommunication challenges. Due to the high information rate and notable distance transmission capacity of fiber optics, the market has been overtaken by this innovation for some time now. Research is showing that fiber optic technology is far superior to metal wire technology. Furthermore, they are resistant to obstruction and experience less signal loss. Fewer dormant states are fundamentally required in many applications, such as cloud computing and algorithmic superconductor exchange.

Prospects

The creation of novel optical devices like solid-state lasers, white light diodes, data storage, optical detectors, radiation detectors, and medical has made REI-doped glasses an intriguing field of research with a broad range of scientific applications, further examination of the studied glasses will however reveal more significant features. The suggested qualities of these glasses that need to be tested for upcoming research include Raman spectroscopy and Nuclear magnetic resonance (NMR) analyses of the structural behavior will provide extensive details about the vibrational band in the studied glasses. The investigation of the dielectric features of the glasses selected will reveal data on the prepared glasses' AC and DC conductivities at various temperatures and frequencies, as well as their dielectric constant. This knowledge is crucial for electronics like solar energy converters.

Conclusions

In summary, this review delved into the photoluminescence and optical properties of rare earth ion-doped glasses. The study utilized spectroscopic techniques, including absorption and luminescence measurements, to assess these properties. By analyzing the absorption spectra, oscillator strengths and Judd-Ofelt intensity parameters were estimated, shedding light on electronic transitions within the glasses. Luminescence measurements further explored radiative characteristics of excited states, non-radiative relaxation processes, and both spontaneous and stimulated emission phenomena. Additionally, the review examined the bonding and electronic structure of the glass matrix through the nephelauxetic effect, bonding parameters, and optical band gaps. Special emphasis was placed on Er^{3+}- doped and Er^{3+}/Yb^{3+}-co-doped glasses, discussing their absorption and emission spectra and the impact of REI environments on hypersensitive transitions. Overall, this review enhances the understanding of photoluminescence and optical properties in REI-doped glasses, offering valuable insights for applications in photonics, lasers, biomedical fields, and optical communication.

Acknowledgment

The authors would like to thank the staff of the Mechanical Engineering Department at Nile University, Nigeria.

Reference

[1] KS Shaaban, EAA Wahab, AA El-Maaref, M Abdelawwad, ER Shaaban, ES Yousef, H Hillmer and J Borcsok. Judd-Ofelt analysis and physical properties of erbium modified cadmium lithium gadolinium silicate glasses. *J. Mater. Sci. Mater. Electron.* 2020; **31**, 4986-96.

[2] KM Goodenough, F Wall and D Merriman. The rare earth elements: Demand, global resources, and challenges for resourcing future generations. *Nat. Resour. Res.* 2018; **27**, 201-16.

[3] V Balaram. *Chapter 4 Sources and applications of rare earth elements. In*: A Sinharoy and PNL Lens (Eds.). Environmental technologies to treat rare earth element pollution: Principles and engineering. IWA Publishing, London, 2010.

[4] KA Naseer and K Marimuthu. The impact of Er/Yb co-doping on the spectroscopic performance of bismuth borophosphate glasses for photonic applications. *Vacuum* 2021; **183**, 109788.

[5] A Limpichaipanit, T Tunkasiri and A Ngamjarurojana. Optical and photocatalytic properties of bismuth vanadate doped bismuth silicate glasses. *Optik* 2019; **182**, 496-9.

[6] AE Ersundu, G Karaduman, M Celikbilek, N Solak and S Aydın. Effect of rare-earth dopants on the thermal behavior of tungsten-tellurite glasses. *J. Alloys Compd.* 2010; **508**, 266-72.

[7] CM Mardziah, S Ramesh, CY Tan, H Chandran, A Sidhu, S Krishnasamy and J Purbolaksono. Zinc-substituted hydroxyapatite produced from calcium precursor derived from eggshells. *Ceram. Int.* 2021; **47**, 33010-9.

[8] S Kaur, OP Pandey, CK Jayasankar and N Chopra. Spectroscopic, thermal and structural investigations of Dy 3 + activated zinc borotellurite glasses and nano-glass-ceramics for white light generation. *J. Non Cryst. Solids* 2019; **521**, 119472.

[9] CM Reddy, BD Prasad, NJ Sushma, NS Dhoble and SJ Dhoble. A review on optical and photoluminescence studies of RE 3 þ (RE ¼ Sm , Dy , Eu , Tb and Nd) ions doped LCZSFB glasses. *Renew. Sustain. Energy Rev.* 2015; **51**, 566-84.

[10] G Huber, C Krankel and K Petermann. Solid-state lasers: Status and future. *J. Opt. Soc. Am. B* 2010; **27**, B93-B105.

[11] U.S. Environmental Protection Agency. *Chapter 11: Mineral products industry.* U.S. Environmental Protection Agency, Washington, 1995.

[12] E Kolobkova, A Alkhlef, N Kuzmenko, IA Khodasevich and A Grabtchikov. NIR and visible luminescence of Er3 +/Yb3+ co-doped fluorophosphate glasses with small additives of phosphates. *J. Lumin.* 2021; **235**, 118033.

[13] SN Kane, A Mishra and AK Dutta. Preface: International conference on recent trends in physics (ICRTP 2016). *J. Phys. Conf. Ser*. 2016; **755**, 011001.

[14] BD Gould, JA Rodgers, M Schuette, K Bethune, S Louis, R Rocheleau and K Swider-Lyons. Performance and limitations of 3D-Printed bipolar plates in fuel cells. *ECS J. Solid State Sci. Tech.* 2015; **4**, P3063-P3068.

[15] GVJ Gowda, C Devaraja, B Eraiah, A Dahshan and SN Nazrin. Structural, thermal and spectroscopic studies of Europium trioxide doped lead boro-tellurite glasses. *J. Alloys Compd.* 2021; **871**, 159585.

[16] A Kaur, A Khanna and LI Aleksandrov. Structural, thermal, optical and photo-luminescent properties of barium tellurite glasses doped with rare-earth ions. *J. Non Cryst. Solids* 2017; **476**, 67-74.

[17] MR Dousti and RJ Amjad. Luminescence enhancement in eu (III) -doped tellurite glass embedded silver nanoparticles. *J. Nanostuct.* 2013; **3**, 435-41.

[18] J Jiang, P Trundle, J Ren, YL Cheng, CY Lee and YL Huang. *Weare intechopen, the world's leading publisher of open access books built by scientists, for scientists TOP 1 %.* IntechOpen Limited, London, 2010.

[19] HC Vasconcelos and AS Pinto. *Fluorescence properties of rare-earth-doped sol-gel glasses.* IntechOpen, London, 2017.

[20] F Sharifianjazi, N Parvin and M Tahriri. Synthesis and characteristics of sol-gel bioactive SiO2-P2O5-CaO-Ag2O glasses. *J. Non Cryst. Solids* 2017; **476**, 108-13.

[21] M Catauro, F Bollino, F Papale and SV Ciprioti. Investigation on bioactivity, biocompatibility, thermal behavior and antibacterial properties of calcium silicate glass coatings containing Ag. *J. Non Cryst. Solids* 2015; **422**, 16-22.

[22] IK Battisha, MA Salem, Y Badr, M Kamal and AMSE Nahrawy. Synthesis and characterization of triply doped nano-composite alumina-phospho- silicates SiO2-P2O5-Al2O3 with Er3+, Sm3+ and Yb3+ ions prepared by sol gel technique in two different forms thin film and monolith. *New J. Glass Ceram.* 2016; **6**, 1-7.

[23] YM Sgibnev, NV Nikonorov and AI Ignatiev. High efficient luminescence of silver clusters in ion-exchanged antimony- doped photo-thermo-refractive glasses: Influence of antimony content and heat treatment parameters. *J. Lumin.* 2017; **188**, 172-9.

[24] P Varak, P Nekvindova, S Vytykacova, A Michalcova, P Malinsky and J Oswald. Near-infrared

photoluminescence enhancement and radiative energy transfer in RE-doped zinc-silicate glass (RE = Ho, Er, Tm) after silver ion exchange. *J. Non Cryst. Solids* 2021; **557**, 120580.

[25] D Singh, S Singh, T Singh and P Kaur. Samarium and gadolinium-co-doped lead borate glasses for luminescent applications. *J. Mater. Sci. Mater. Electr.* 2021; **32**, 6900-11.

[26] S Rakpanich, P Meejitpaisan and J Kaewkhao. Physical, optical and luminescence properties of Er3+-doped bismuth borosilicate glasses. *Key Eng. Mater.* 2016; **675**, 372-5.

[27] SA Umar, MK Halimah, KT Chan and AA Latif. Physical, structural and optical properties of erbium doped rice husk silicate borotellurite (Er-doped RHSBT) glasses. *J. Non Cryst. Solids* 2017; **472**, 31-8.

[28] SL Meena. Thermal and physical properties of Pm 3+ ions doped lead lithium bismuth silicate glasses. *J. Pure Appl. Ind. Phys.* 2019; **9**, 72-81.

[29] V Hegde, A Wagh, H Hegde, CSD Vishwanath and SD Kamath. Spectroscopic investigation on europium doped heavy metal borate glasses for red luminescent application. *Appl. Phys. A* 2017; **12**, 302.

[30] MD Hassib, KM Kaky, A Kumar, E Sakar, MI Sayyed, SO Baki and MA Mahdi. Boro-silicate glasses co-doped Er+3/Yb+3 for optical amplifier and gamma radiation shielding applications. *Phys. B Condens. Matter* 2019; **567**, 37-44.

[31] I Khan, G Rooh, R Rajaramakrishna, N Srisittipokakun, HJ Kim, K Kirdsiri and J Kaewkhao. Luminescence characteristics of Sm^{3+} -doped lithium barium gadolinium silicate glasses for Orange LED's. *Spectrochim. Acta Part A Mol. Biomal. Spectrosc.* 2019; **214**, 14-20

[32] MHM Zaid, HAA Sidek, R El-Mallawany, KA Almasri and KA Matori. Synthesis and characterization of samarium doped calcium soda-lime-silicate glass derived wollastonite glass-ceramics. *J. Mater. Res. Tech.* 2020; **9**, 13153-60.

[33] RF Muniz, VO Soares, GH Montagnini, AN Medina and ML Baesso. Thermal, optical and structural properties of relatively depolymerized sodium calcium silicate glass and glass-ceramic containing CaF2. *Ceram. Int.* 2021**; 47**, 24966-72.

[34] SN Nazrin, MK Halimah, FD Muhammad, JS Yip, L Hasnimulyati, MF Faznny, MA Hazlin and I Zaitizila. The effect of erbium oxide in physical and structural properties of zinc tellurite glass system. *J. Non Cryst. Solids* 2018; **490**, 35-43.

[35] A Acikgoz, G Ceyhan, B Aktas, Yalcin S and G Demircan. Luminescent, structural and mechanical properties of erbium oxide doped natural obsidian glasses. *J. Non Cryst. Solids* 2021; **572**, 121104.

[36] NAN Razali, IS Mustafa, NZN Azman, HM Kamari, AA Rahman, K Rosli, NS Taib and NA Tajuddin. The physical and optical studies of erbium doped borosilicate glass. *J. Phys. Conf. Ser.* 2018; **1083**, 012004.

[37] AM Hamza, MK Halimah, FD Muhammad and KT Chan. Physical properties, ligand field and Judd-Ofelt intensity parameters of bio- silicate borotellurite glass system doped with erbium oxide. *J. Lumin.* 2019; **207**, 497-506.

[38] YB Saddeek, ER Shaaban, ES Moustafa and HM Moustafa. Spectroscopic properties, electronic polarizability, and optical basicity of Bi2O3-Li2O-B2O3 glasses. *Phys. B Condens. Matter* 2008; **403**,

2399-407.

[39] K Mariselvam, RA Kumar and VR Rao. Concentration-dependence and luminescence studies of erbium doped barium lithium fluoroborate glasses. *Opt. Laser Tech.* 2019; **118**, 37-43.

[40] K Swapna, S Mahamuda, AS Rao, M Jayasimhadri, T Sasikala and LR Moorthy. Optical absorption and luminescence characteristics of Dy3+ doped Zinc Alumino Bismuth Borate glasses for lasing materials and white LEDs. *J. Lumin.* 2013; **139**, 119-24.

[41] KF Herzfeld. On atomic properties which make an element a metal. *Phys. Rev.* 1927; **29**, 701-5.

[42] MK Halimah, MF Faznny, MN Azlan and HAA Sidek. Optical basicity and electronic polarizability of zinc borotellurite glass doped La^{3+} ions. *Results Phys.* 2017; **7**, 581-9.

[43] I Kashif, A Ratep and G Adel. Polarizability, optical basicity and optical properties of $SiO_2B_2O_3Bi_2O_3TeO_2$ glass system. *Appl. Phys. A* 2018; **124**, 486.

[44] V Dimitrov and S Sakkav. Linear and nonlinear optical properties of simple oxides. *J. Appl. Phys.* 1996; **79**, 1741-5.

[45] V Dimitrov and T Komatsu. An interpretation of optical properties of oxides and oxide glasses in terms of the electronic ion polarizability and average single bond strength. *J. Univ. Chem. Tech. Metall.* 2010; **45**, 219-50.

[46] MN Azlan, MK Halimah, SZ Shafinas and WM Daud. Polarizability and optical basicity of Er^{3+} ions doped tellurite based glasses. *Chalcogenide Lett.* 2014; **11**, 319-35.

[47] US Aliyu, HM Kamari, IG Geidam, IO Alade, AM Noorazlan, AM Hamza and AF Ahmad. Spectroscopic investigations of Er_2O_3 doped silica borotellurite glasses. *Opt. Mater.* 2021; **114**, 110987.

[48] G Chandrashekaraiah, VCV Gowda, A Jayasheelan, CN Reddy and KJ Mallikarjunaiah. Correlation among the oxide ion polarizability, optical basicity and interaction parameter in Gd^{3+} ions doped oxyhalide borate glasses. *J. Phys. Conf. Ser.* 2021; **2070**, 012050.

[49] AA El-Maaref, EAA Wahab, KS Shaaban and RM El-Agmy. Enhancement of spectroscopic parameters of Er3+-doped cadmium lithium gadolinium silicate glasses as an active medium for lasers and optical amplifiers in the NIR-region. *Solid State Sci.* 2021; **113**, 106539.

[50] JA Duffy and MD Ingram. An interpretation of glass chemistry in terms of the optical basicity concept. *J. Non Cryst. Solids* 1976; **21**, 373-410.

[51] E Moustafa and F Elkhateb. The estimation of the oxide ion Polarizability for B_2O_3-Li_2O-Mo Glass System 232. *Am. J. Appl. Sci.* 2012; **9**, 446-9.

[52] RR Reddy, YN Ahammed, PA Azeem, KR Gopal and TVR Rao. Electronic polarizability and optical basicity properties of oxide glasses through average electronegativity. *J. Non Cryst. Solids* 2001; **286**, 169-80.

[53] M Deepa, R Doddoji, CSD Viswanath and AV Chandrasekhar. Optical and NIR luminescence spectral studies: Nd^{3+}-doped borosilicate glasses. *J. Lumin.* 2019; **213**, 191-6.

[54] CR Kesavulu, HJ Kim, SW Lee, J Kaewkhao, N Wantana, S Kothan and S Kaewjaeng. Influence of Er^{3+} ion concentration on optical and photoluminescence propoped gadolinium-calcium silica borate glasses. *J. Alloys Compd.* 2016; **683**, 590-8.

[55] MS Sadeq and HY Morshidy. Effect of mixed rare-earth ions on the structural and optical properties of some borate glasses. *Ceram. Int.* 2019; **45**, 18327-32.

[56] CR Kesavulu, HJ Kim, SW Lee, J Kaewkhao, E Kaewnuam and N Wantana. Luminescence properties and energy transfer from Gd^{3+} to Tb^{3+} ions in gadolinium calcium silicoborate glasses for green laser application. *J. Alloys Compd.* 2017; **704**, 557-64.

[57] N Razali, FA Musa, N Jumadi and AY Jalani. Production of calcium oxide from eggshell: Study on calcination temperature, raw weight and contact time. *RSU Int. Res. Conf.* 2021; **624**, 624-37.

[58] M Zagrai, RC Suciu,V Rada, ME Pica and S Pruneanu. Structural and optical properties of Eu^{3+} ions in lead glass for photonic applications. *J. Non Cryst. Solids* 2021; **569**, 120988.

[59] K Mariselvam, RA Kumar and S Karthik. Optical and luminescence characteristics of europium doped barium lithium fluoroborate glasses. *Chem. Phys.* 2019; **525**, 110379.

[60] BK Kumar, PR Babu, E Kavaz, YK Kshetri, T Kim, VDCD Anjos and BDP Raju. Spectroscopic characteristics and gain cross-section profiles of erbium-doped boro-tellurite glasses for optical amplifier applications. *Opt. Mater.* 2024; **148**, 114950.

[61] R Wan, C Guo, X Li and P Wang. Spectroscopic properties and numerical analysis of novel erbium doped multi-component tellurite glasses. *Ceram. Int.* 2024; **50**, 7168-76.

[62] F Zaman, G Rooh, N Chanthima, SU Khan, HJ Kim, S Kothan, N Chanlek, M Ashad and J Kaewhao. Investigation of spectroscopic and photoluminescence properties of Erbium doped phosphate (P2O5-K2O3-Al2O3) glasses. *J. Alloys Compd.* 2022; **893**, 162215.

[63] EM Bouabdalli, M El-Jouad, S Touhtouh, A Chellakhi and A Hajjaji. Synthesis, structural, and optical behavior of erbium-doped silicophosphate glasses for photonics applications. *Luminescence* 2024; **39**, 4802.

[64] S Hraiech, C Bouzidi and M Ferid. Luminescence properties of Er^{3+}-doped phosphate glasses. *Phys. B Condens. Matter* 2017; **522**, 15-21.

[65] MHA Mhareb, S Hashim, SK Ghoshal, YSM Alajerami, MA Saleh, MMA Maqableh and N Tamchek. Optical and erbium ion concentration correlation in lithium magnesium borate glass. *Optik* 2015; **126**, 3638-43.

[66] AS Asyikin, AA Latif, MK Halimah, MHM Zaid, MA Kamarudin, MF Faznny, SN Nazrin and I Zaitizila. Structural and optical properties of samarium doped silica borotellurite glasses for optical switching application. *Opt. Laser Tech*. 2024; **168**, 109857.

[67] M Shwetha, B Eraiah and Roopa. Physical and optical properties of samarium doped sodium lithium phosphate glasses. *AIP Conf. Proc.* 2023; **2399**, 020009.

[68] S Mohan, S Kaur, DP Singh and P Kaur. Structural and luminescence properties of samarium doped lead alumino borate glasses. *Opt. Mater.* 2017; **73**, 223-33.

[69] Y Tayal and AS Rao. Orange color emitting Sm^{3+} ions doped borosilicate glasses for optoelectronic device applications. *Opt. Mater.* 2020; **107**, 110070.

[70] Z Zhao, B Zhang, Y Gong, Y Ren, M Huo and Y Wang. Concentration effect of Yb^{3+} ions on the spectroscopic properties of high-concentration Er^{3+} / Yb^{3+} co-doped phosphate glasses. *J. Mol. Struct.* 2020; **1216**, 128322.

[71] University of Alabama at Birmingham, Available at: https://people.cas.uab.edu/~vfedorov/Notes/Judd%20Ofelt%20theory.pdf, accessed.

[72] N Deopa, B Kumar, MK Sahu, PR Rani and AS Rao. Effect of Sm^{3+} ions concentration on borosilicate glasses for reddish orange luminescent device applications. *J. Non Cryst. Solids* 2019; **513**, 152-8.

[73] R Vijayakumar and K Marimuthu. Concentration-dependent spectroscopic properties of Sm^{3+} doped borophosphate glasses. *J. Mol. Struct.* 2015; **1092**, 166-75.

[74] YA Tanko, SK Ghoshal and MR Sahar. Ligand fi eld and Judd-Ofelt intensity parameters of samarium doped tellurite glass. *J. Mol. Struct.* 2016; **1117**, 64-8.

[75] W Luo, J Liao, R Li and X Chen. Determination of judd - ofelt intensity parameters from the excitation spectra for rare-earth doped luminescent materials. *Phys. Chem. Chem. Phys.* 2010; **12**, 3276-82.

[76] G Lakshminarayana, M Mao, R Yang, JR Qiu and MG Brik. Spectroscopic investigations of Nd^{3+}-, Er^{3+}-, Er^{3+}/Yb^{3+}-, and Tm^{3+}-ions doped SiO2-Al2O3-CaF2-GdF3 glasses. *Phys. B Condens. Matter* 2009; **404**, 3348-55.

[77] MAFAA Elbakey and MKEl Mansy. Judd – Ofelt and spectroscopic analysis of erbium ions co-doped with samarium ions in phosphate glasses environment. *Opt. and Quat. Elect.* 2023; **55**, 1-16.

[78] S Liu, G Zhao, Y Li, H Ying, J Wang and G Han. Optical absorption and emission properties of Er^{3+} doped mixed alkali borosilicate glasses. *Opt. Mater.* 2008; **30**, 1393-8.

[79] O Ravi, CM Reddy, L Manoj and BDP Raju. Structural and optical studies of Sm^{3+} ions doped niobium borotellurite glasses. *J. Mol. Struct.* 2012; **1029**, 53-9.

[80] VS Bhagavan, R Ravanamma, KV Krishnaiah, N Ravi, UK Kagola, CR Kesavulu, PL Saranya, and V Venkatramu. Orange-red luminescence of samarium-doped bismuth–germanium–borate glass for light-emitting devices. *Lumt.* 2023; **38**, 1750-57.

[81] SG Arelli, A Kumar and SJ Dhoble. Characterization of luminescence of samarium with phosphate Compounds. *Mater. Today Proc*. 2020; **27**, 649-51.

[82] C Basavapoornima, T Maheswari, S Rani and CK Jayasankar. Sensitizing effect of Yb^{3+} ions on photoluminescence properties of Er^{3+} ions in lead phosphate glasses. Optical fiber amplifiers. *Opt. Mater.* 2018; **86**, 256-69.

[83] K Nasser, V Aseev, S Ivanov, A Ignatiev and N Nikonorov. Spectroscopic and laser properties of erbium and ytterbium co-doped photo-thermo-refractive glass. *Ceram. Int. 2*020; **46**, 26282-8.

[84] W Rittisut, N Wantana, Y Ruangtaweep, P Mool-Am-Kha, S Rujirawat, P Manyum, R Yimnirun, P Kidkhunthod, A Prasatketragarn, S Kothan, HJ Kim and J Kaekhao. The radioluminescence and photoluminescence behavior of lithium alumino borate glasses doped with Tb_2O_3 and Gd_2O_3 for green luminescence applications. *Opt. Mater.* 2021; **121**, 111437.

[85] P Yasaka and J Kæwkhao. White emission materials from glass doped with rare Earth ions: A review. *AIP Conf. Proc.* 2016; **1719**, 020002.

[86] L Mishra, A Sharma, AK Vishwakarma, K Jha, M Jayasimhadri, BV Ratnam, K Jang, AS Rao and RK Sinha. White light emission and color tunability of dysprosium doped barium silicate glasses. *J. Lumin.* 2016; **169**, 121-7.

[87] R Vijayakumar, G Venkataiah and K Marimuthu. Structural and luminescence studies on Dy^{3+} doped

boro-phosphate glasses for white LED's and laser applications. *J. Alloys Compd.* 2015; **652**, 234-43.

[88] K Jha and M Jayasimhadri. Structural and emission properties of Eu^{3+}-doped alkaline earth zinc-phosphate glasses for white LED applications. *J. Am. Ceram. Soc.* 2017; **100**, 1402-11.

[89] R Borges, JF Schneider and J Marchi. Structural characterization of bioactive glasses containing rare earth elements (Gd and/or Yb). *J. Mater. Sci.* 2019; **54**, 11390-9.

[90] K Srigurunathan, R Meenambal, A Guleria, D Kumar, JMDF Ferreira and S Kannan. Unveiling the effects of rare-earth substitutions on the structure, mechanical, optical, and imaging features of ZrO_2 for Biomedical applications. *ACS Biomater. Sci. Eng.* 2019; **5**, 1723-43.

[91] Y Zhang, M Hu, W Zhang and X Zhang. Research on rare earth doped mesoporous bioactive glass nanospheres. I. Similarity of *in vitro* biological effects. *J. Non Cryst. Solids* 2022; **587**, 121586.

[92] M Ershad, A Ali, NS Mehta, RK Singh, SK Singh and R Pyare. Mechanical and biological response of (CeO2+La2O3)-substituted 45S5 bioactive glasses for biomedical application. *J. Aust. Ceram. Soc.* 2020; **56**, 1243-52.